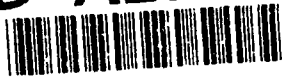# NAVAL POSTGRADUATE SCHOOL
Monterey, California

AD-A257 506

DTIC
ELECTE
DEC 01 1992
S A D

92-30438

THESIS

Thermal Cycling Behavior of Unidirectional and Cross-plied

P100 Gr/6061 Aluminum Composites

by

Anthony D. Wiest

September 1992

Thesis Advisor: Indranath Dutta
Co-Advisor: Shantanu Mitra

REPORT DOCUMENTATION PAGE

1a. REPORT SECURITY CLASSIFICATION UNCLASSIFIED	1b. RESTRICTIVE MARKINGS
2a. SECURITY CLASSIFICATION AUTHORITY	3. DISTRIBUTION/AVAILABILITY OF REPORT
2b. DECLASSIFICATION/DOWNGRADING SCHEDULE	Approved for public release; distribution is unlimited

4. PERFORMING ORGANIZATION REPORT NUMBER(S)	5. MONITORING ORGANIZATION REPORT NUMBER(S)

6a. NAME OF PERFORMING ORGANIZATION Naval Postgraduate School	6b. OFFICE SYMBOL (if applicable) 69	7a. NAME OF MONITORING ORGANIZATION Naval Postgraduate School
6c. ADDRESS (City, State, and ZIP Code) Monterey, CA 93943-5000		7b. ADDRESS (City, State, and ZIP Code) Monterey, CA 93943-5000

8a. NAME OF FUNDING/SPONSORING ORGANIZATION	8b. OFFICE SYMBOL (if applicable)	9. PROCUREMENT INSTRUMENT IDENTIFICATION NUMBER
8c. ADDRESS (City, State, and ZIP Code)		10. SOURCE OF FUNDING NUMBERS

PROGRAM ELEMENT NO.	PROJECT NO.	TASK NO.	WORK UNIT ACCESSION NO.

11. TITLE (Include Security Classification)
THERMAL CYCLING BEHAVIOR OF UNIDIRECTIONAL AND CROSS-PLIED P100 GR/6061 ALUMINUM COMPOSITES

12. PERSONAL AUTHOR(S)
Wiest, Anthony, D.

13a. TYPE OF REPORT Master's Thesis	13b. TIME COVERED FROM _____ TO _____	14. DATE OF REPORT (Year, Month, Day) 1992, September	15. PAGE COUNT 58

16. SUPPLEMENTARY NOTATION The views expressed in this thesis are those of the author and do not reflect the official policy or position of the Department of Defense or the United States Government.

17. COSATI CODES			18. SUBJECT TERMS (Continue on reverse if necessary and identify by block number)
FIELD	GROUP	SUB-GROUP	aluminum-graphite composite, thermal strain response, thermal cycling

19. ABSTRACT (Continue on reverse if necessary and identify by block number)
The thermal strain response of as-cast samples of 40% P100 graphite fiber reinforced 6061 Al composites in the unidirectionally reinforced and the [0/90] cross-plied configuration was studied. Thermal strain hysteresis and residual plastic strain were observed, both changing with continued cycling. The compressive residual plastic strain is attributable primarily to creep deformation due to compressive residual stress in the matrix at elevated temperature. The role of matrix creep in the heating rate dependence of the strain response was studied by measuring strains under isothermal conditions in the absence of applied stresses. Damage mechanisms operative in the composites during thermal cycling, and the impact of ply constraint on the strain response were also evaluated.

20. DISTRIBUTION/AVAILABILITY OF ABSTRACT [X] UNCLASSIFIED/UNLIMITED [ ] SAME AS RPT. [ ] DTIC USERS	21. ABSTRACT SECURITY CLASSIFICATION UNCLASSIFIED
22a. NAME OF RESPONSIBLE INDIVIDUAL Indranath Dutta, Prof., Material Science Dept, NPS	22b. TELEPHONE (Include Area Code) (408) 646-2581 22c. OFFICE SYMBOL ME/DU

DD FORM 1473, 84 MAR   83 APR edition may be used until exhausted   SECURITY CLASSIFICATION OF THIS PAGE
All other editions are obsolete   UNCLASSIFIED

i

Thermal Cycling Behavior of Unidirectional and Cross-plied P100 Gr/6061 Aluminum Composites

by
Anthony D. Wiest
Lieutenant, United States Coast Guard
B.S., United States Coast Guard Academy, 1984

Submitted in partial fulfillment of the
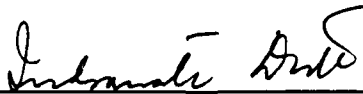requirements for the degree of

MASTER OF SCIENCE IN MECHANICAL ENGINEERING
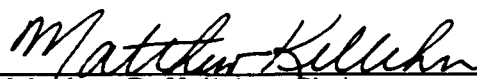
from the

NAVAL POSTGRADUATE SCHOOL
September, 1992

Author: _____
Anthony D. Wiest

Approved By: _____
Indranath Dutta, Thesis Advisor

_____
Shantanu Mitra, Thesis Co-Advisor

_____
Matthew D. Kelleher. Chairman
Department of Mechanical Engineering

ABSTRACT

The thermal strain response of as-cast samples of 40% P100 graphite fiber reinforced 6061 Al composites in the unidirectionally reinforced and the [0/90] cross-plied configuration was studied. Thermal strain hysteresis and residual plastic strain were observed, both changing with continued cycling. The compressive residual plastic strain is attributable primarily to creep deformation due to compressive residual stress in the matrix at elevated temperature. The role of matrix creep in the heating rate dependence of the strain response was studied by measuring strains under isothermal conditions in the absence of applied stresses. Damage mechanisms operative in the composites during thermal cycling, and the impact of ply constraint on the strain response were also evaluated.

Accesion For		
NTIS CRA&I		☑
DTIC TAʒ		☐
Unannounced		☐
Justification		
By		
Distribution /		
Availability Codes		
Dist	Avail and / or Special	
A-1		

TABLE OF CONTENTS

I. INTRODUCTION

The study of composite materials is a relatively new area in materials science research. Although crude composites such as the adobe brick existed long ago, it was not until the early 1960s that the current study of advanced composite materials originated [Ref. 1]. The driving need for the development of composite materials was due to design criteria which traditional monolithic metals and alloys could not meet [Ref. 2]. High tech applications in the aerospace industry and the military were the initial impetus for research and design of composite materials. Today the scope of application of composites has spread to the automotive and construction industries as well as into the manufacturing of recreational sporting equipment.

Metal matrix composites (MMCs) typically consist of a soft, ductile matrix metal which surrounds a hard, stronger reinforcing component. The form of the reinforcement can be small spherical particles or fibers. Most of the research to date has focused on continuous fiber composites. Continuous fiber MMCs offer processing advantages not found in monolithic metals. These advantages allow tailoring the mechanical and thermal properties of the composite to meet specific design requirements. This flexibility in achieving the desired properties is controlled by several important factors:

1. selection of the metal matrix and fiber
2. volume percentages of matrix and fiber
3. interfacial bonding between fiber and matrix
    a. wetting agents
    b. fiber diameter and volume fraction
4. manufacturing temperature
5. stacking sequence of lamina

Manufacturing processes for MMCs are typically diffusion bonding or casting. Since both of these are elevated temperature processes, there are residual stresses which build up in the composite upon cooling from the manufacturing temperature.

due to the difference in coefficients of thermal expansion (CTEs) between the graphite fiber and the aluminum matrix. In the case of Al-Gr composites the substantial difference in the CTEs make the residual stresses quite large. The magnitude of the residual stress which occurs after manufacturing is dependent upon the CTE difference and the interfacial bonding between the fiber and the matrix metal. As will be discussed later in this work, the residual stresses present in the composite affect the thermal expansion behavior exhibited by the composite as it undergoes thermal cycling.

To promote bonding between the fibers and the matrix, the fibers are typically coated with a wetting agent. In the casting process the coated fibers are then drawn into tows, aligned in the proper orientations, and infiltrated by the liquid metal matrix material. If the fiber density is not too large and is evenly distributed, then the liquid metal can easily infiltrate the fiber tows and produce the desired end product. However, as the fiber density increases the infiltration process becomes more difficult. This can lead to voids forming within the composite, thereby weakening the bonding interface due to less contact area between the fiber and matrix.

Aluminum-graphite (Al-Gr) continuous fiber reinforced MMCs have material characteristics which make them good candidates where high strength-to-weight and high modulus-to-weight ratios are necessary. In addition, the excellent thermal conductivity exhibited and the ability to design the composite with a very small coefficient of thermal expansion (CTE) lends the use of Al/Gr MMCs to applications where heat removal and dimensional stability are critical.

Various agencies within the Navy, such as the Naval Surface Warfare Center (Crane) and the Naval Air Warfare Center (Indianapolis) are considering using cross-plied [0/90] Al-Gr MMCs (6061 Al/P100 Thornel) with 40% volume fraction as the mounting frame for electronic modules because of the low-density, high-

stiffness, and high thermal conductivity properties. While each of the properties mentioned is important to the overall performance of the composite for this particular application, it is the study of the thermal strain response of the composite that is investigated in this work.

II. LITERATURE SURVEY

A. THERMAL RESIDUAL STRESSES OF MMC

Due to the large differences in CTEs between the aluminum matrix and the graphite fibers, thermal residual stresses are induced in the composite as it cools from manufacturing temperature to room temperature. While the CTE of the aluminum matrix is isotropic, that of the graphite fiber is not. The CTEs for the materials used in this study are as follows:

1. 6061 aluminum, $\alpha_{Al} = 23 \times 10^{-6}/°C$

2. P100 graphite. $\alpha_{Gr(Long)} = -0.9 \times 10^{-6}/°C$

3. P100 graphite, $\alpha_{Gr(Trans)} = 9.4 \times 10^{-6}/°C$

Much previous work has been done on investigating the nature and magnitude of the residual stress present in the composite at room temperature. It is well documented and easily hypothesized, that in unidirectional Al-Gr composites the thermal residual stress in the fiber direction is tensile in the aluminum matrix and compressive in the fiber [Ref. 3]. Figure 2.1 shows a conceptual thermal excursion depicting the stresses induced upon cooling from the manufacturing temperature [Ref. 4]. The residual stresses present after manufacturing will affect the way in which the composite responds to mechanically applied loads and to thermally induced stresses.

Because of the anisotropic nature of the fiber there is very little difference between the transverse CTE of the fiber and that of the aluminum matrix. This would seem to result in a much smaller buildup of stresses in the transverse direction upon cooling. However, Tsai et al. [Ref. 5], using x-ray diffractometry to measure stresses

4

Fabrication
Temperature

Gr   Al

(a)

Room
Temperature

Gr   Al

(b)

Room
Temperature

Gr   Al

(cut to shape)
(c)

⟶ = Longitudinal stress

— — — — — = Schematic of lattice planes, showing
distortion due to residual stresses
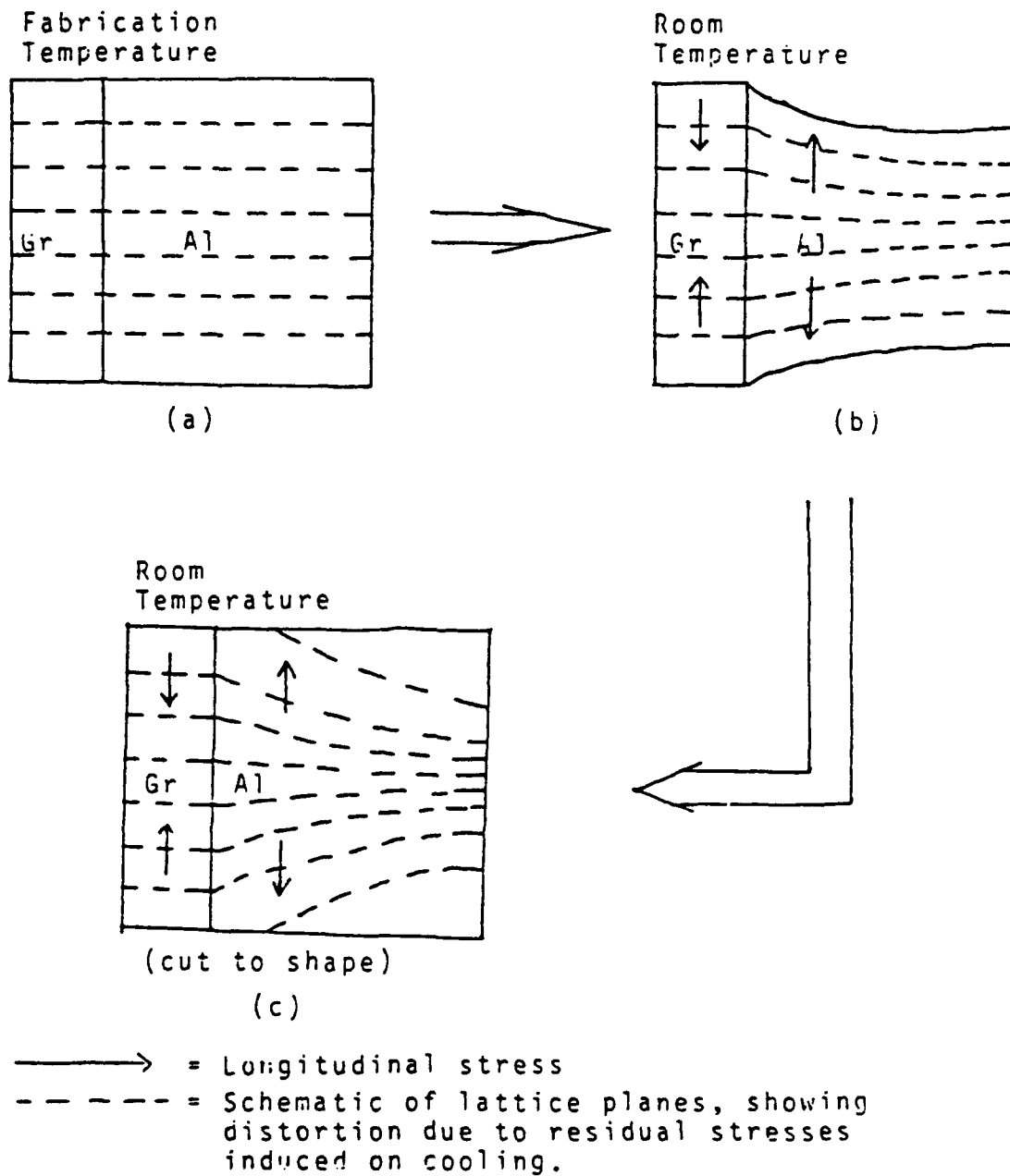induced on cooling.

**Figure 2.1 : A conceptual thermal excursion undergone by a small section
of the matrix adjacent to a fiber in an MMC during manufacturing.
Figure c is after cutting to make fiber ends and matrix flush. [Ref.4]**

in a 201 Al/P50 MMC, also found tensile stresses of considerable magnitude in the transverse direction. This was attributed to mechanical effects (Poisson's effect).

While many researchers have investigated the residual stress state of the unidirectionally reinforced MMC, the cross-plied MMC has not been as extensively examined. However, it was deduced by Mitra et al. [Ref. 6], that if residual stresses were tensile in nature in the longitudinal and transverse directions of the unidirectionally reinforced MMC, then by cross plying laminae, the stress in both directions would still remain tensile although the magnitude would be altered. It seems logical that as the number of cross-plied layers is increased, the residual stress state should approach equal magnitudes in the longitudinal and transverse directions.

Since the residual stress state will affect the strain response of the MMC under mechanical and thermal loading, alteration of the residual stress state has been investigated by methods of both heat treatment and cryogenic treatment. The intent of these treatments is to reduce the stress present in the composite to achieve a more uniform strain response under various loading conditions.

Tsai [Ref. 5] found that by subjecting the composite to liquid nitrogen temperatures, and then allowing it to return to room temperature, a reduction in the stress magnitude of approximately 30 percent was obtained.

Park [Ref. 7], who also used X-ray techniques and observed tensile residual stresses present in a unidirectional 6061 Al/P100 Gr MMC, found that after quenching in liquid nitrogen a compressive residual stress was generated.

B. RESIDUAL STRESS EFFECTS UPON THERMAL CYCLING

Typical features which are observed when thermally cycling Al/Gr MMCs are strain hysteresis between the heating and cooling segments of the thermal cycle and a residual plastic strain which occurs at the end of the cycle.

Dries and Tompkins [Ref. 8] observed a large tensile residual strain after one thermal cycle of P100 Gr/6061 Al between 250°F and -250°F. In subsequent cycles the residual plastic strain disappeared, however thermal strain hysteresis continued to exist. They believed the hysteresis was due to induced stresses exceeding the elastic limit of the matrix during the thermal cycle. By post-consolidation processing, which consisted of a solution heat treatment, room temperature water quench, artificial aging, and finally a cryogenic treatment, they showed th⌐ʳ the thermal strain hysteresis could be significantly reduced.

Wolff et al. [Ref. 9] also attributed the major cause of thermal hysteresis to matrix plasticity occurring over the thermal cycle, and further hypothesized that finer control over the matrix properties could reduce the dimensional changes of the composite.

Tompkins and Dries [Ref. 10] also showed that the thermal history can affect the strain response of the composite. They cycled samples of P100 Gr/6061 Al over a range of temperatures from 130 K to 408 K. The CTE at the end of this cycle was positive. By reversing the thermal cycle and going from room temperature to 408 K to 130 K and back to room temperature, the CTE at the end of the cycle was zero or slightly negative. Subsequent heating of the first sample would cause an expansion, however heating the second sample would cause no expansion and possibly even a contraction to occur.

The CTE of the composite has also been correlated to matrix plasticity by several researchers. Kural and Min [Ref. 11] plotted theoretical strain vs. temperature curves for cycling of a P100/Az91C Mg lamina between a range of temperatures from 150°F to -150°F. The theoretical CTE of the lamina was observed to be very near that of the fiber as cooling from room temperature to -150°C occurred. This was attributed to tensile yielding of the matrix almost immediately upon cooling. Once

matrix plasticity was induced, the strain response was dominated by the elastic fibers.

In addition to thermal strain hysteresis and residual plastic strains which occur because of the residual stresses, the strain response of the composite is also dependent on the thermal cycling rate. This is due to stress relaxation mechanisms which become operative at higher temperatures in the thermal cycle. Several researchers including Wolff et al. [Ref 9], Koss and Copley [Ref. 12] and Garmong [Ref. 13], have indicated that the strain response is rate dependent.

C. DAMAGE DUE TO THERMAL CYCLING

Exposure to cyclical temperature profiles causes the residual stresses generated within the composite to fluctuate. The severity of the temperature range, and the number of thermal cycles completed, will both affect the subsequent strain response of the composite. The different behavior exhibited between early cycles and later cycles, of a composite subjected to such testing, can primarily be attributed to damage accumulation over the course of cycling.

Khan [Ref. 14] showed that prolonged exposure above temperatures of 500°C caused the formation of Al_4C_3 to form at the aluminum-graphite interfaces. This formation of Al_4C_3 was shown to cause degradation of the fiber strength, and hence a corresponding degradation in the overall strength of the composite. Prolonged exposures to temperatures below 500°C did not show the formation of Al_4C_3.

Zong et al. [Ref. 15] have shown, during in situ thermal cycling of an Al/Gr MMC in a scanning electron microscope (SEM), the extent of fiber intrusion and extrusion occurring over the course of a thermal cycle from room temperature to 300°C. As expected, upon heating fiber intrusion begins to occur, followed by a return to the initial state as the composite is cooled to room temperature. Repeated thermal cycles would be expected to increase the magnitude of the intrusion and ex-

trusion observed as the debonded length of the interface near the ends of the sample increases.

D. RESEARCH OBJECTIVES

From previous research a better understanding of the residual stress state of the MMC and alterations to this stress state via heat or cryogenic treatments has been obtained. The strain response of the unidirectionally reinforced MMC has also been previously examined during thermal cycling, and correlations between the thermal strain response and the residual stress state of the composite constituents have been made. Additionally, micrographic observations have shown damage occurring to the interfaces between the fiber and matrix which results in a loss of composite strength.

This work attempts to increase the understanding of the Al/Gr MMC by investigating the thermal strain response of unidirectional and cross-plied MMCs subjected to different thermal rates. Damage modes occurring at each rate are also investigated by micrographic observations conducted prior to, and after thermal cycling. In addition, the rate dependence of the thermal strain response for the unidirectionally reinforced MMC is investigated, by observing the strain behavior under isothermal conditions, after various heating rates were used to reach this temperature.

III. EXPRIMENTAL PROCEDURES

A. MATERIALS AND NOMENCLATURE

The material studied in this research consisted of an as-cast, P100 Thornel graphite fiber, 40 volume percent, 6061 aluminum MMC. Two different samples of this material were obtained from Fiber Materials Incorporated, Bitterford, ME. The first sample consisted of unidirectional fiber reinforcement. The second sample consisted of a four-ply [0/90], fiber orientation. By making the appropriate cuts in the unidirectional composite a sample could be obtained with reinforcing fibers either parallel (**longitudinal**), or perpendicular (**transverse**) to the measurement axis. These orientations are shown in Figure 3.1. Likewise, from the four-ply material a 0/90/90/0 (**LTTL**) or a 90/0/0/90 (**TLLT**) orientation could be obtained. These orientations are shown in Figure 3.2. Throughout the remainder of this work the orientations shown in these figures will be used to identify the experimental specimens.

B. THERMAL STRAIN MEASUREMENT

An Orton™ automatic recording dilatometer was used to measure the thermal strain of the Al-Gr composite. The output from the dilatometer, which was in millivolts, was reduced using a Hewlett Packard data acquisition unit, model 3852A. A copy of the data acquisition program is included in the appendix. This data was then entered into Macintosh computer to allow plotting of the strain vs. temperature and strain vs. time curves presented in the experimental results section.

The unidirectionally reinforced MMC and the four-ply MMC both had a nominal thickness of 2.0 mm. Samples prepared for dilatometry experiments were cut to a rectangular shape measuring approximately 26 mm long by 6 mm wide. The
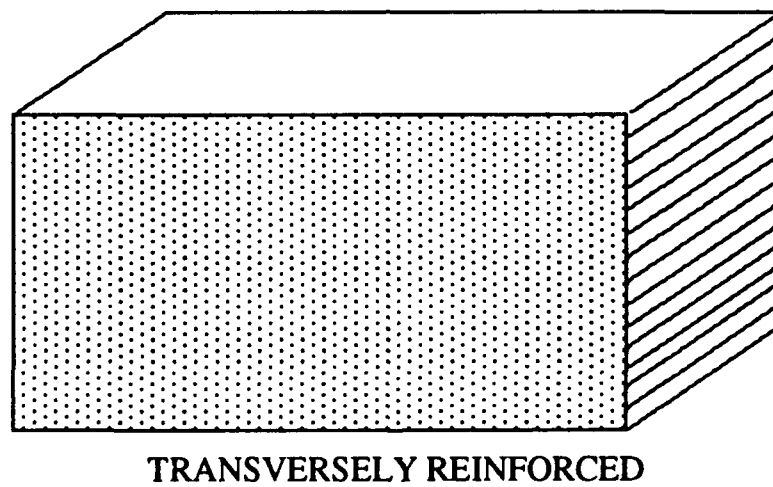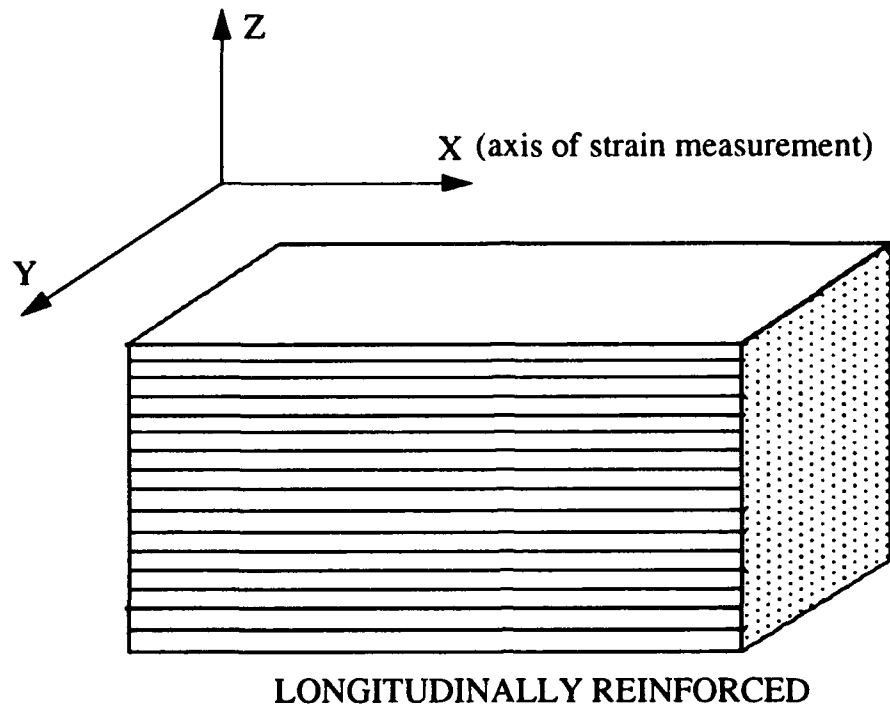
Figure 3.1 : Unidirectionally reinforced MMCs showing the longitudinally and transversely reinforced orientations. Measurement of strain was along the X-axis.
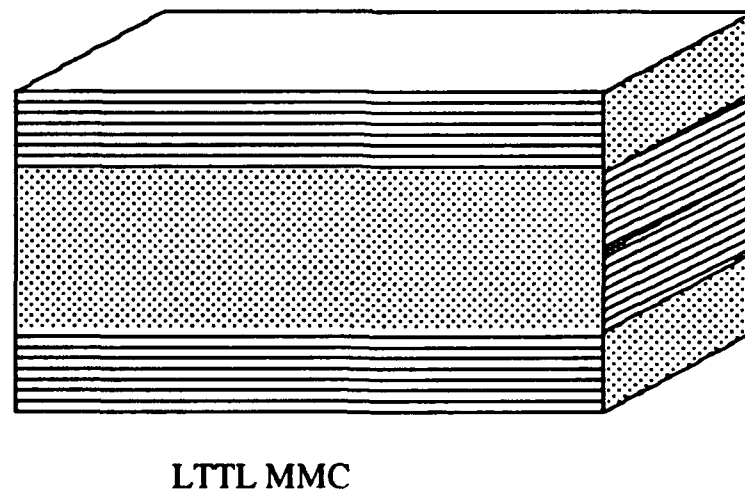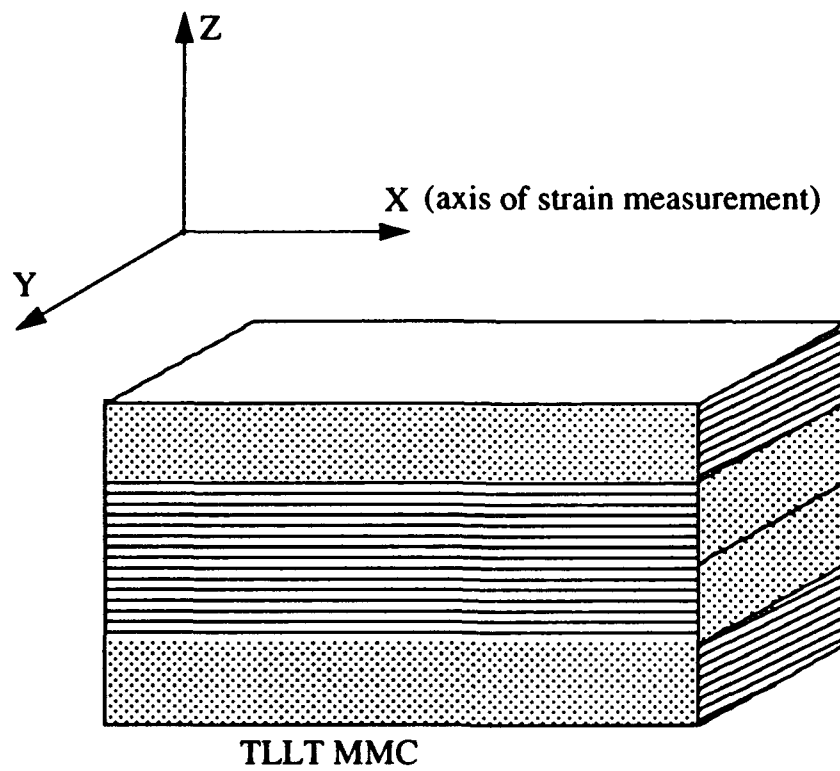
Figure 3.2 : Four-ply MMCs showing the TLLT and the LTTL orientations. Measurement of strain was along the X-axis.

edges of the samples were then sequentially sanded using 240, 320, 400 and 600 grit sand paper. The sample-ends were rounded and the edges were beveled as shown in Figure 3.3. The final sample size was approximately 25.4 mm long and 5.5 mm wide.
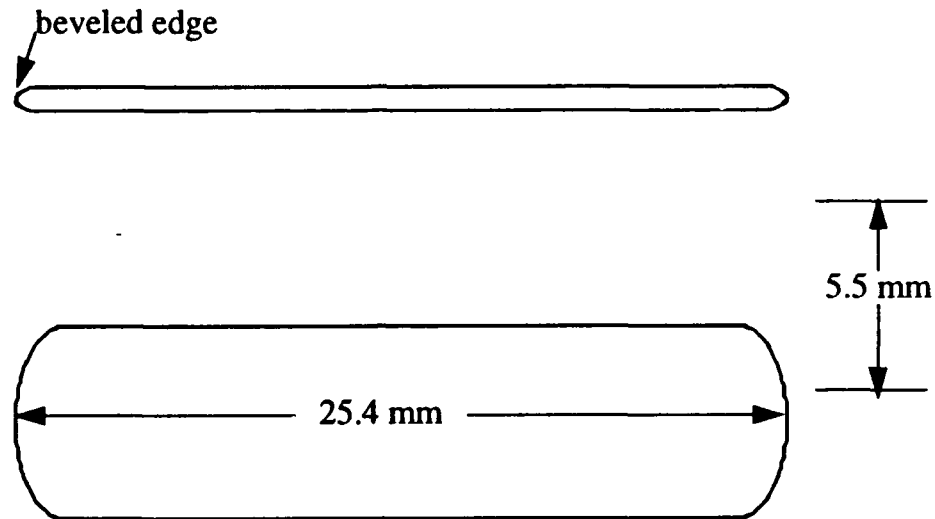

Figure 3.3 : Schematic of samples used for dilatometry experiments.

The initial thermal cycling rates used when measuring strain vs. temperature were 0.89°C/min during the heating segment, followed by 0.25°C/min during the cooling segment. All cycling was conducted in an argon atmosphere. Strain vs. temperature plots for all four sample orientations previously shown were obtained at these rates for the first, second and tenth thermal cycles over a range of temperatures from room temperature to 540°C.

A much slower heating rate of 0.15°C/min was used on the unidirectional, longitudinally reinforced MMC to investigate the dependency of the strain response on the thermal cycling rate. The cooling rate remained unchanged. A strain vs. temperature plot for the unidirectional, longitudinally reinforced MMC was

obtained at these rates for the first and second thermal cycles over a range of temperatures from room temperature to 100°C.

The final experiments with which the dilatometer was used to measure the isothermal creep strain, consisted of heating samples at various rates until an isothermal holding temperature was reached. Once the isothermal holding temperature was achieved, the thermal strain occurring at the temperature was recorded. This allowed a strain vs. time plot to be generated. This experiment was performed only on the unidirectional, longitudinally reinforced MMC.

C. RAPID THERMAL CYCLING

Samples for each of the orientations of Figure 3.1 and Figure 3.2 were prepared as shown in Figure 3.3 and then cycled nine times at a heating and cooling rate of 17.33°C/min to 540°C in an argon atmosphere. A schematic of the apparatus used for cycling is shown in Figure 3.4.
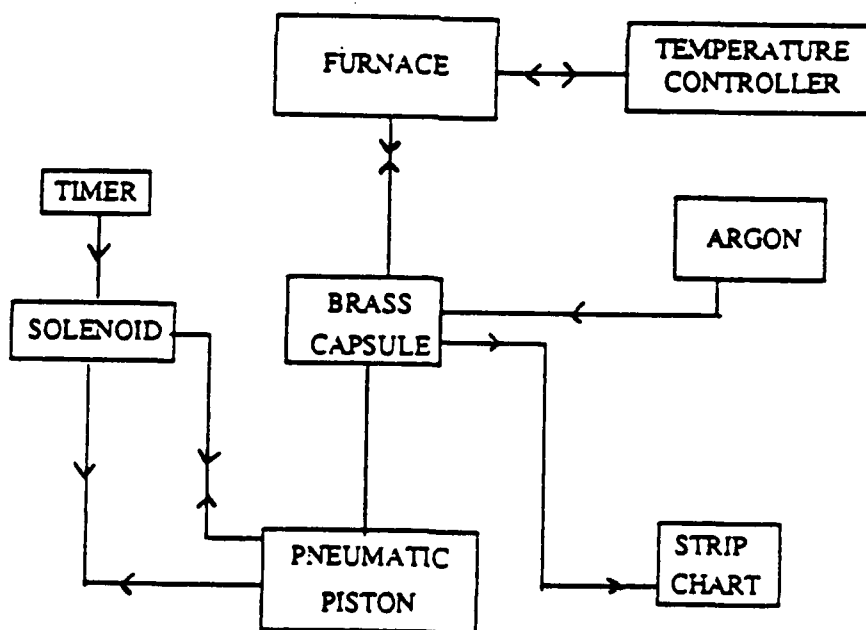
Figure 3.4 :Schematic of the apparatus used to thermally cycle samples.

The cycling apparatus used consisted of a pneumatic piston which was controlled by a solenoid valve connected to a Chontrol digital timer. A brass capsule was fitted to the end of the piston to hold the sample and to allow an inert atmosphere to be maintained. A chromel-alumel, type K, thermocouple was inserted into the brass capsule so that actual sample temperatures could be recorded by a strip chart recorded.

The brass capsule assembly was then cycled into a Marshall tube furnace, model 1134, which was being maintained at a uniform, predetermined temperature. After a 30 minute period the desired maximum temperature was achieved and the piston assembly was cycled out of the furnace. The actual temperature profile over the course of one thermal cycle is shown in Figure 3.5.
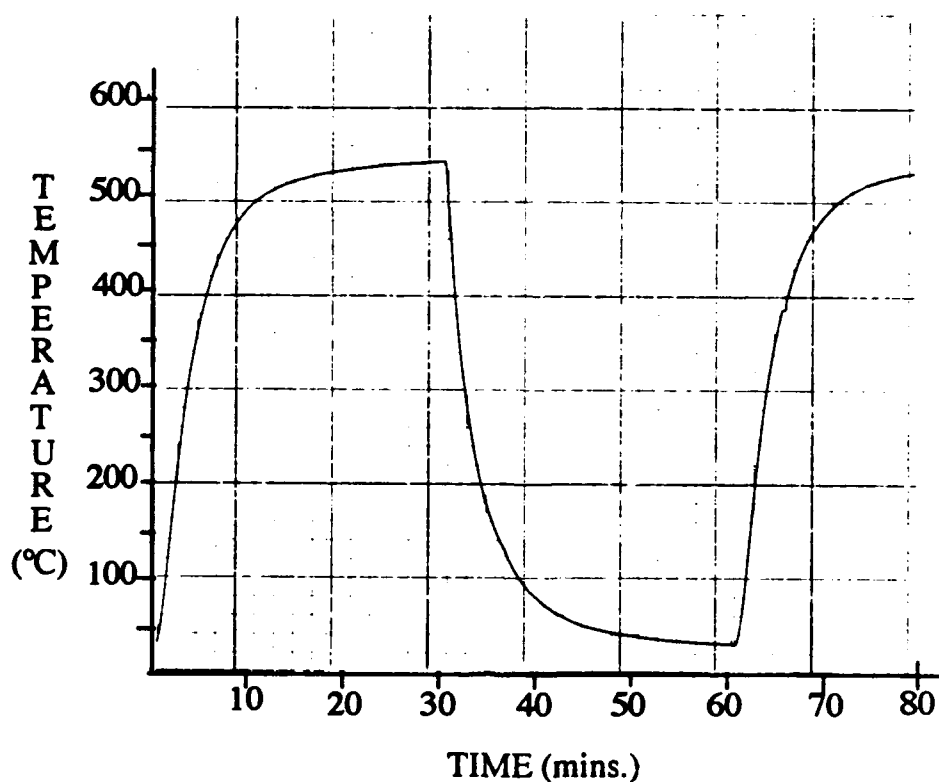

Figure 3.5 : Temperature profile of the rapidly cycled MMCs.

15

After nine cycles were performed at the rapid cycling rate, the sample was removed from the brass capsule and placed into the dilatometer. Strain measurements were then taken over the tenth thermal cycle at the heating rate of $0.89°C/min$ and the cooling rate $0.25°C/min$. Strain vs. temperature plots for the tenth heating cycle were then compared for the sample which had received ten slow cycles and the sample which had nine rapid cycles and one slow cycle.

D. MICROSCOPY OF THERMALLY CYCLED SAMPLES

Micrographic observations of the MMCs were conducted in the Scanning Electron Microscope (SEM). Sample-ends were observed in the as-received condition, after one thermal cycle to $540°C$ and after ten cycles to $540°C$.

The unidirectional, longitudinally reinforced samples, which had experienced ten slow cycles, and which had experienced nine rapid cycles and one slow cycle, were sectioned near the sample-end. The cross-sectioned area was then polished, receiving a final polish with 0.05 micron alumina suspension. These cross sections were then examined in the SEM to determine the extent and type of internal interfacial damage which had occurred over the different thermal histories of the two samples.

IV. EXPERIMENTAL RESULTS

A. STRAIN RESPONSE OF THE UNIDIRECTIONALLY REINFORCED MMC CYCLED TO 540°C

A low magnification micrograph of the unidirectionally reinforced MMC (obtained by backscattered electron imaging in the SEM) is shown in Figure 4.1 below. It is apparent that the fiber distribution throughout the cross-section of the sample is nonuniform. As mentioned previously, the fiber distribution may affect the strain response of the composite. Since the fiber distributions in the experimental composites were not totally uniform, accurate comparisons between the strain response of different composite samples is not attempted in this work.
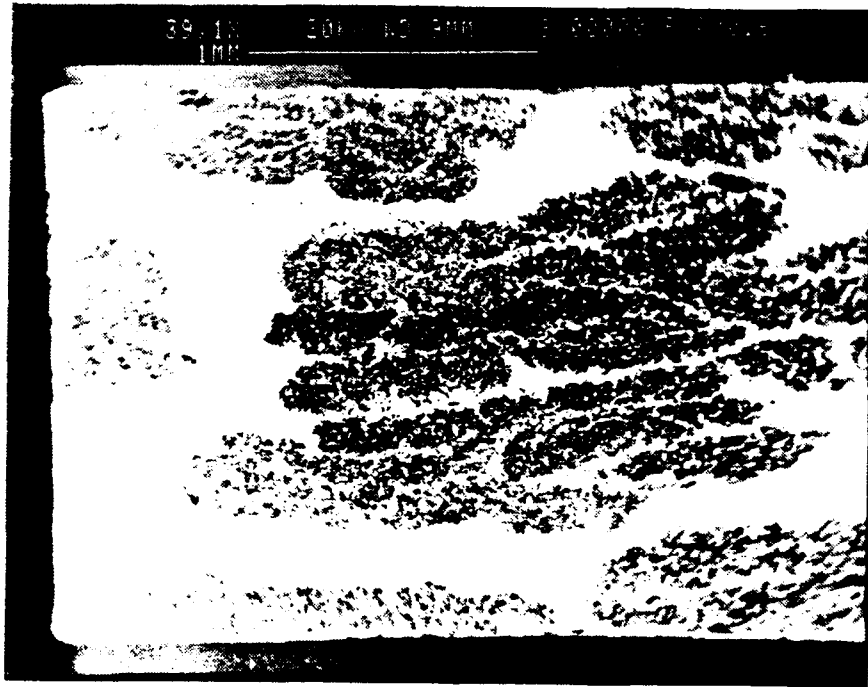
Figure 4.1: Low magnification micrograph of unidirectionally reinforced MMC.

1. Longitudinal Fiber Orientation

a. Dilatometry Experiments

Figure 4.2 shows the strain vs. temperature curves for a sample cycled twice between room temperature and 540°C at a heating rate of 0.89°C/min and a cooling rate of 0.25°C/min. Several features are immediately apparent. A significant strain hysteresis exists between the heating and cooling segments of each cycle and also a residual compressive strain exists at the end of each thermal cycle. Additionally, the compressive residual strain decreases in magnitude from the first to the second cycle.

Figure 4.2 : Thermal strain response of the unidirectionally reinforced MMC during the first and second thermal cycles.

18

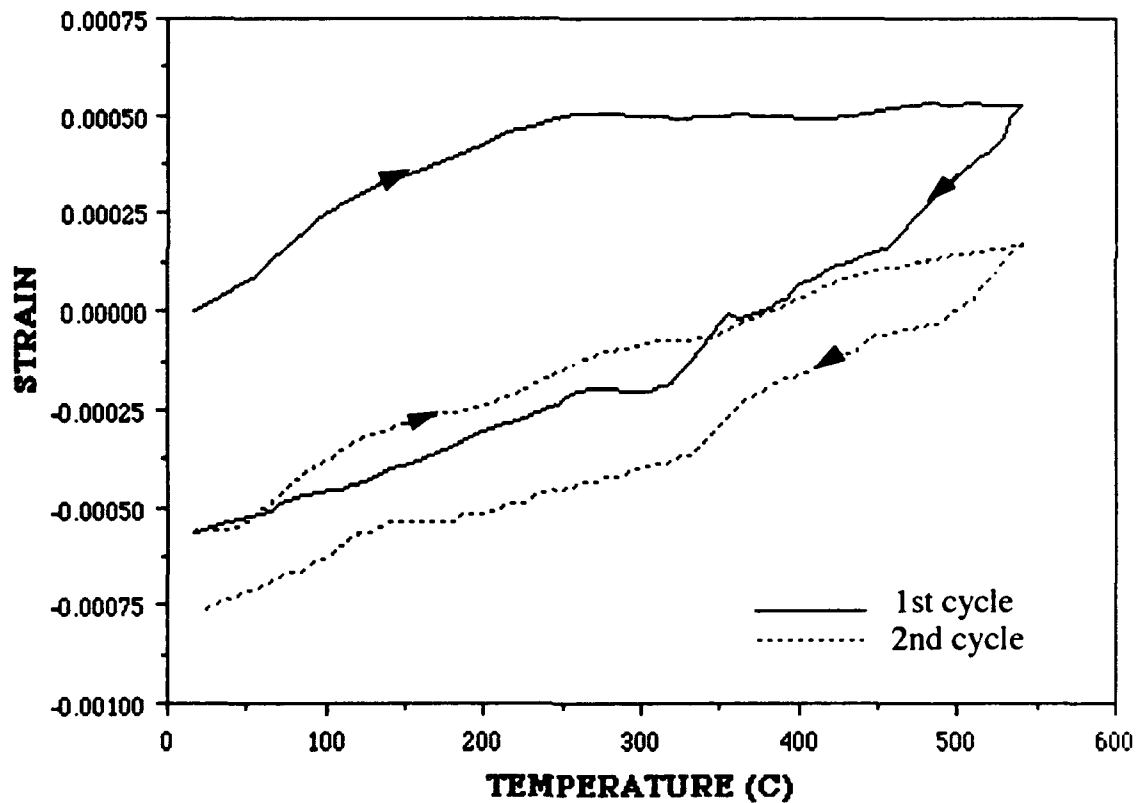The explanation for this behavior is as follows. Upon initial heating from room temperature the residual tensile stress which is present in the matrix aids the expansion of the composite. In the 50-100°C range the calculated value of the CTE is approximately $3.5 \times 10^{-6}/°C$. This is larger than the CTE value of $2.0 \times 10^{-6}/°C$ obtained from a simple rule of mixtures calculation. This is due, in part, to the tensile residual stress present in the matrix, and in part due to fabrication-related effects.

Further heating causes the residual tensile stress to continuously decrease until the composite reaches a stress-free state. The exact point of this stress-free state is not known. However, when the slope of the curve is approximately equal to the theoretical CTE, the residual stresses in the composite are small enough in magnitude not to have a significant effect on the strain response. This stress-free or low-stress region probably occurs between the temperatures of 120-230°C (the region in which the CTE ~ $2 \times 10^{-6}/°C$). As the temperature rises above 230°C the compressive stress induced in the composite by the contraction of the graphite fibers is large enough to flatten the strain response and to limit further extension of the composite through the remainder of the heating segment. This zero CTE is due to several factors. The fibers are now inducing a compressive stress in the matrix and this opposes normal expansion of the MMC. In addition, the compressive stress coupled with the elevated temperature may lead to compressive matrix creep and/or compressive yielding due to reduction of the matrix yield strength at higher temperatures.

Due to the stress relieving effects of compressive creep and plastic deformation, the compressive stress at 540°C does not build to a very large magnitude. Upon initial cooling from 540°C the compressive stress aids in the contraction of the MMC. This stress is quickly relieved and tensile stresses again

19

build in the matrix until room temperature. After the first thermal cycle a large compressive residual plastic strain is noted and is attributed to the effects of compressive creep and/or compressive yielding which occur in the higher temperature regime of the first heating segment.

The second heating cycle has similar characteristics as the first to a temperature of 250°C. At this temperature the slope of the first cycle flattens, however the second cycle slope remains unchanged. This difference is due to the compressive stresses above 250°C not being as large in magnitude in the second cycle as in the first. This can only be due to a larger tensile residual stress present at the start of the second cycle. This larger tensile stress may be attributed to the strain hardening of the matrix which occurs over the first thermal cycle, thereby allowing a larger tensile stress to build as the composite cools to room temperature. This is also supported by the decrease in the magnitude of the compressive residual plastic strain after the second cycle from that of the first. Although it would appear that plastic deformation/creep at the higher temperatures would result in recrystallization of the matrix, the presence of the reinforcing fibers serves to stabilize a subgrain structure that results from recovery, never really allowing recrystallization to occur. This leads to an overall increase in the dislocation density in the matrix resulting in a higher residual stress after the first thermal excursion. This large residual stress state, which is tensile, is relieved at higher temperatures during the second cycle than during the first, leading to less compressive creep over the second cycle and smaller compressive plastic strain.

To investigate damage mechanisms which may depend on the thermal cycling rate, the strain response of a slowly cycled (0.89°C/min) sample was compared with that of a rapidly cycled (17.35°C/min) sample after nine cycles. For both samples, the strain response of the tenth cycle was measured by heating at 0.89°C/min and cooling at 0.25°C/min. This comparison is shown in Figure 4.3.

Before an explanation of the figure is given it is important to note two differences between the first cycle shown in Figure 4.2 and the tenth slow cycle shown below. First, the residual strain magnitude after ten slow cycles is significantly larger, and second the temperature at which the zero slope region is reached is higher (~325°C, as compared to 250°C in the first cycle). Both of these features are indications of damage accumulation during thermal cycling and will be discussed later.
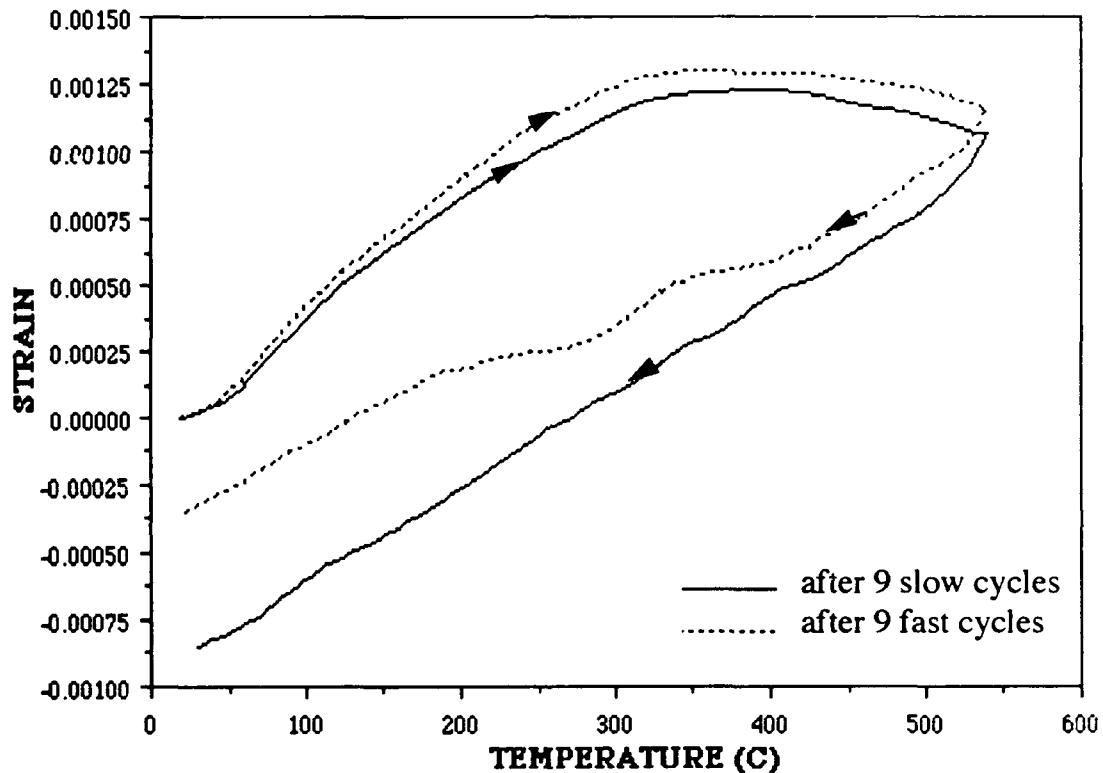

Figure 4.3 : Thermal strain response during the tenth cycle of the unidirectionally reinforced MMC following nine slow cycles (0.89°C /min, heating; 0.25°C /min, cooling) and nine fast cycles(17.33°C /min, heating and cooling).

The significant feature observed between the two samples is the difference in magnitude of the residual compressive strain existing at the end of the cycle. The slow cycled sample shows a much larger compressive strain. This difference is attributed to the type of damage occurring at the two thermal rates used in this study and will be discussed in the following section.

b. Micrographic Investigation of Damage In Unidirectionally Reinforced MMC

A SEM micrograph of the as-received unidirectionally reinforced composite is shown in Figure 4.4 below. The final polish was done with 0.05 micron alumina suspension. The fiber-matrix interface appears intact in most regions with some infiltration problems occurring in areas with tight fiber bundles.
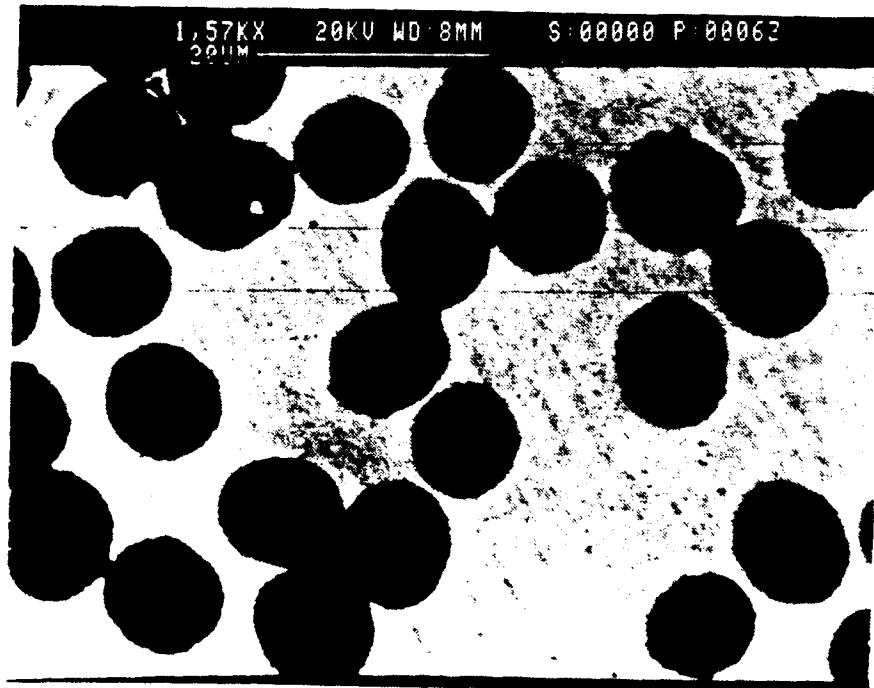
Figure 4.4 : As-received unidirectionally reinforced MMC (1.57 KX).

A similar polish was given to another unidirectionally reinforced specimen which subsequently underwent one slow thermal cycle from room temperature to 540°C and back to room temperature. The SEM micrograph for this sample is shown in Figure 4.5.
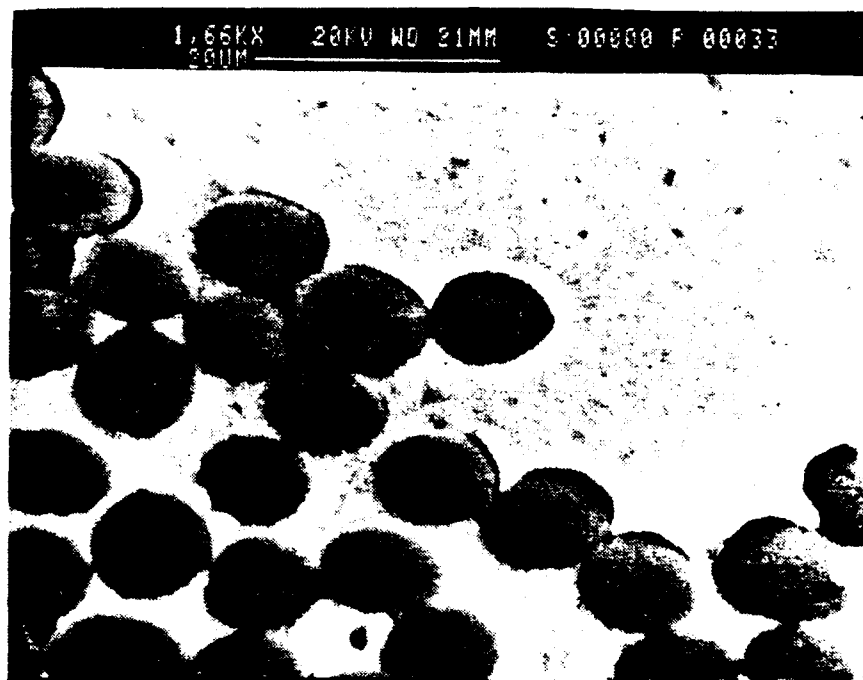
Figure 4.5 : Unidirectionally reinforced MMC after one slow cycle to 540°C (1.66KX).

Not much notable damage is apparent after one slow cycle, however near areas of low fiber concentration (as shown in the upper right hand corner of Figure 4.5), there appears to be some fiber intrusion near the edge of the fiber cluster. This is an unusual effect since any interface damage should release the tensile stress state in the matrix and allow the matrix to locally shrink to an unstressed state. The

23

extrusion of the aluminum matrix near the fiber edges can be explained by tensile plastic yielding of the matrix in regions where it is unconstrained followed by interface failure. This results in fiber intrusion in regions of unconstrained matrix expansion. Similar effects were shown by Zong et al. [Ref 15] who attributed the fiber intrusion to localized stresses.

The strain response in the tenth cycle for both the slowly and the rapidly cycled specimens were similar in form; however, it was suspected that different damage mechanisms may be operative in the two samples, resulting in the difference in residual plastic strains observed in Figure 4.3. To investigate this hypothesis, polished edges of the samples were examined in the SEM after ten cycles. Shown in Figure 4.6 is the slowly cycled sample after ten cycles. The fibers are protruding beyond the matrix by nearly 20 microns, and no damage to the matrix is observed. This is indicative of extensive interfacial failure.

Figure 4.6 : Unidirectionally reinforced MMC after ten slow cycles.

The sample-end was then cut off and the remaining cross section was polished using 0.05 micron alumina suspension. Figure 4.7 shows the cross section of the slowly cycled sample. A feature which is apparent is the radial cracking of many of the fibers. This radial cracking of the fiber is a stress relief mechanism which is induced by the Poisson effect. Tsai et al. [Ref. 5] have previously shown that a considerable residual tensile stress is present in the transverse direction of a P50 Thornel fiber reinforced Al/Gr MMC. During the first few cycles, the transverse
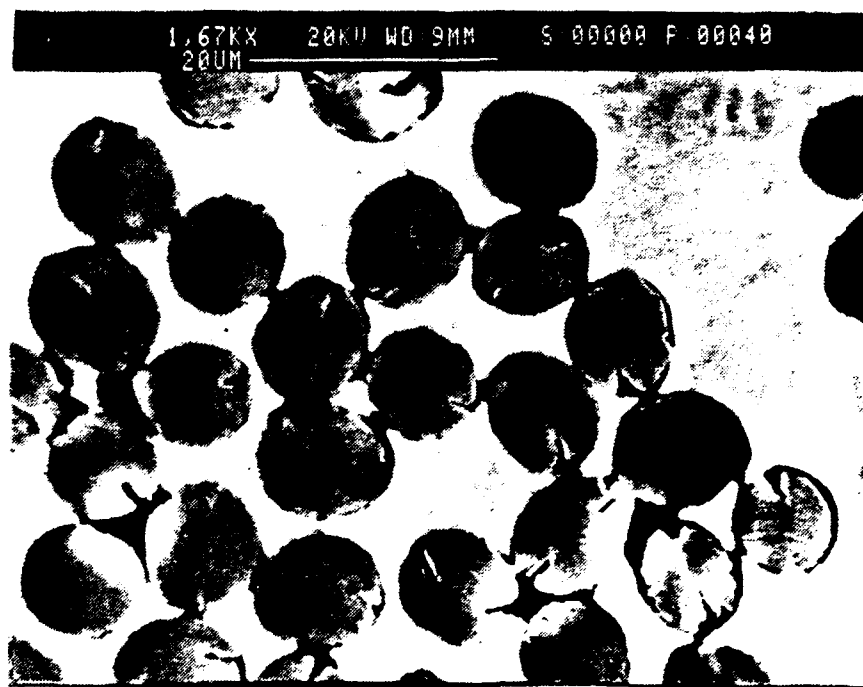

Figure 4.7 : Polished cross section of the unidirectionally reinforced MMC after ten slow cycles(1.67KX).

residual stresses in the matrix and the fiber build up in a manner similar to that described for longitudinal stresses earlier. It is possible that at this stage, the transverse stresses in the fiber exceed the transverse fiber strength, resulting in fiber

25

cracking as seen in Figure 4.7. At some locations, the tensile transverse stress exceeds the transverse strength of the interface and fiber/matrix debonding occurs. During subsequent slow cycles prolonged exposure to temperatures > 500°C (39 hours) can result in the formation of Al_4C_3 at the interface. This drops the interfacial shear strength causing the effect seen in Figure 4.6. It is likely that the interfacial failure seen in Figure 4.6 is an end effect due to the large shear stresses developed at the end during cycling.

Figure 4.8 shows the polished cross section of the fast cycled sample after nine fast cycles and one slow cycle. There is no evidence of radial fiber cracking and there does not appear to be any significant interfacial debonding.
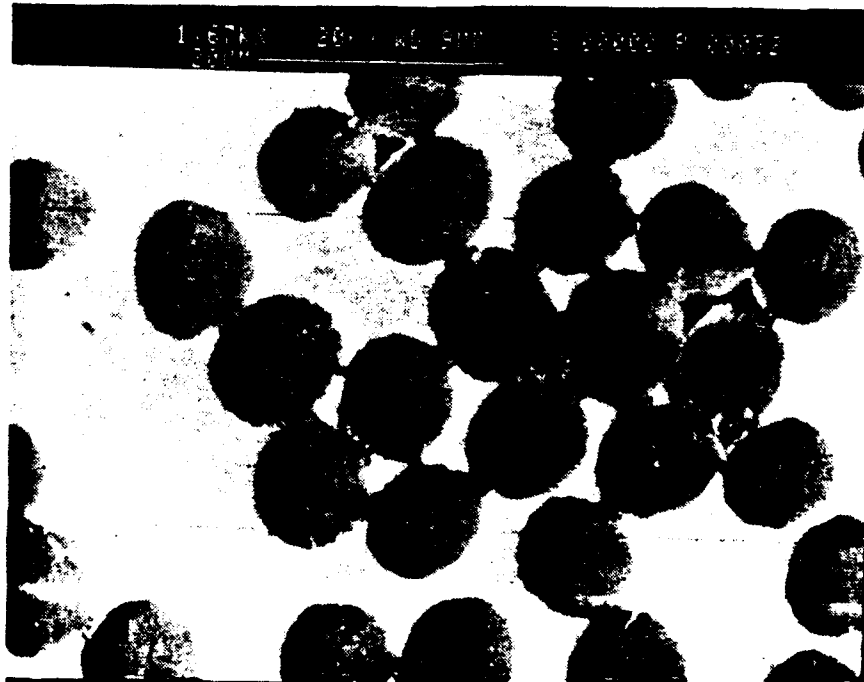

Figure 4.8 : Polished cross section of the unidirectionally reinforced MMC after nine fast and one slow cycle (1.67KX).

26

While the transverse cuts made on both the slowly cycled and the rapidly cycled specimens were made in the same approximate location, this was not a finely measured distance from the end of the sample. The possibility exists that this radial damage could be a local effect which was obscured in the rapidly cycled specimen.

Figures 4.9a and 4.9b are SEM micrographs of the unidirectionally reinforced sample after nine rapid cycles to 540°C and one slow cycle. The damage modes observed in these figures, (i.e., interfacial failure and transverse fiber cracking, followed by crack linking via matrix failure) are different from that observed in the slowly cycled sample (Figure 4.6). Due to the rapid cycling, the time spent above 500°C is minimal, thus precluding the formation of the Al_4C_3. This results in appreciably less interfacial failure, which is mostly confined to small lengths near the sample-end. In addition to this interface failure, we also see some transverse fiber cracking. Eventually these disconnected micro-cracks can link up via matrix failure. This feature is seen only in the rapidly cycled sample because the extent of interfacial shear in this sample is much less than that in the slowly cycled sample, thus allowing the stress and the stress intensity factor ($K = f(\sigma, a)$; a = crack length) in the matrix to reach a level required for matrix failure. In summary the damage in the slowly cycled sample occurs primarily in mode II (interface shear) whereas in the rapidly cycled sample, damage occurs both in mode I (matrix cracking) and mode II.

2. Transverse Fiber Orientation

The unidirectionally reinforced MMC sample with the transverse fiber orientation shows thermal response behavior which is similar to a sample prepared from monolithic 6061 aluminum. The measured CTE of this sample is greater than

(a)
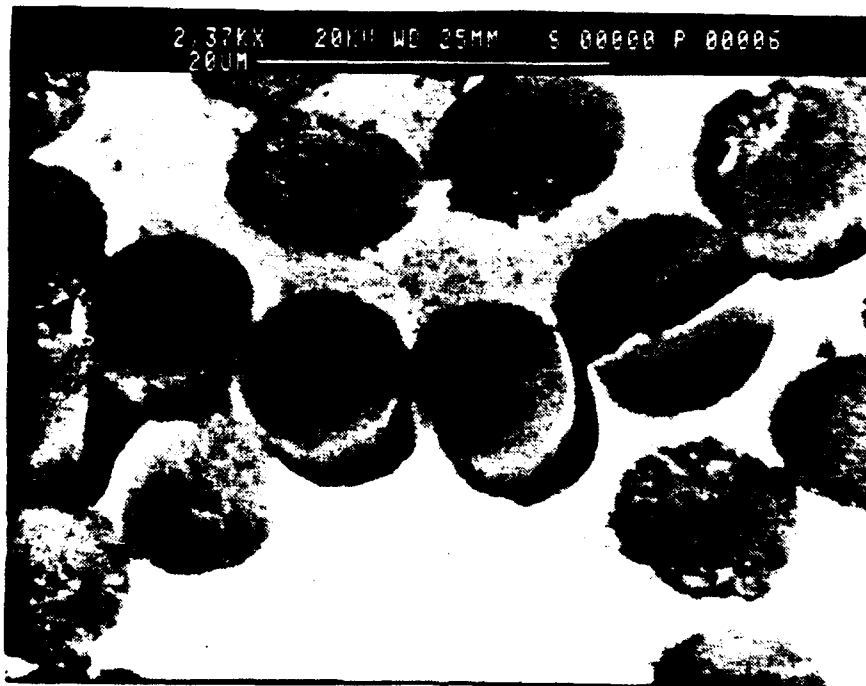
(b)

Figure 4.9 a. and 4.9 b.:Unidirectionally reinforced MMC after nine fast cycles and one slow cycle.

that of 6061 aluminum. This agrees with the findings of Tsai et al. [Ref. 5] who showed that a tensile residual stress was also present in the transverse direction. This stress would aid expansion of the composite, resulting in a higher CTE than that of the monolith. The first and second thermal cycles are shown in Figure 4.10.

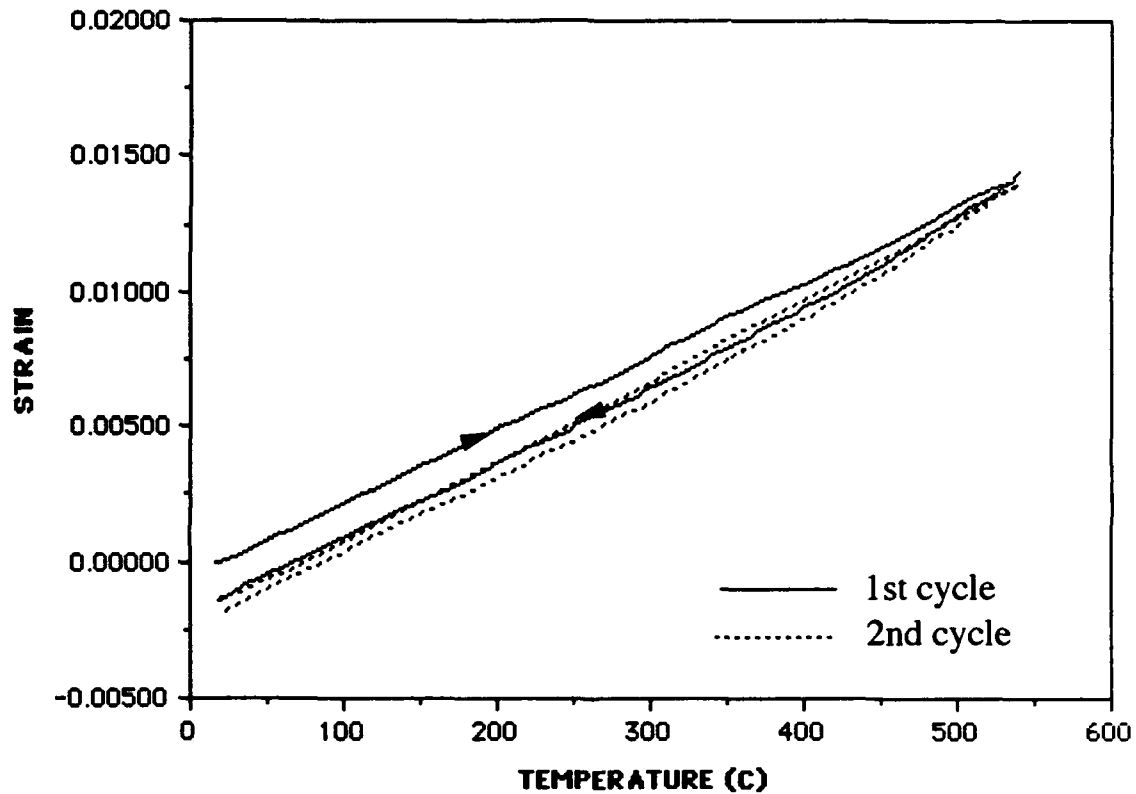**Figure 4.10 : Thermal strain response of the unidirectionally reinforced MMC with transversely oriented fibers during the first and second thermal cycles.**

It is observed that after the first cycle, a compressive residual plastic strain remains. Along the axial direction of the fibers, a tensile residual stress is present as outlined earlier. While heating, this stress gets relieved and a compressive stress

begins to build up, resulting in compressive plastic deformation at high temperatures. This axial compressive deformation would result in a transverse matrix expansion (due to the Poisson effect), aiding the expansion of the MMC at the higher temperatures and yielding a higher CTE over that temperature range. This is observed in Figure 4.10 which shows a slightly larger CTE at temperatures greater than 450°C than at temperatures less than 450°C. During this transverse expansion of the matrix compressive stresses get generated in the matrix along the transverse direction (perpendicular to the fiber axes) since the matrix expansion is constrained by the presence of the fibers which have a different modulus and Poisson's ratio (v) from those of the matrix. This compressive stress can result in some compressive creep of the matrix yielding the small residual strain observed after cycling in Figure 4.10.

Figure 4.11, on the following page, shows the tenth thermal cycle after nine slow and nine rapid cycles respectively. The tenth cycle after nine slow cycles, appears similar to the first cycle (Figure 4.10), while the tenth cycle after rapid cycling shows no residual plastic strain. This can be attributed to the absence of matrix creep along the transverse fiber direction and the consequent absence of transverse compressive stresses due to the Poisson effect in the rapidly cycled sample.

B. STRAIN RESPONSE OF THE FOUR-PLY MMC CYCLED TO 540°C

Due to the cross plying of lamina in the four-ply MMC the additional effect of ply constraint must be considered when explaining the strain response. Furthermore, the stacking sequence of the plies would also be expected to change the response due to a change in the ply constraints. The two stacking sequences examined in this study are identified by the orientation of the plies. TLLT therefore represents the sample with top and bottom lamina containing transversely oriented fibers and the

two middle plies having longitudinally oriented fibers. The LTTL orientation has longitudinally oriented top and bottom lamina with two transversely oriented lamina in the middle.
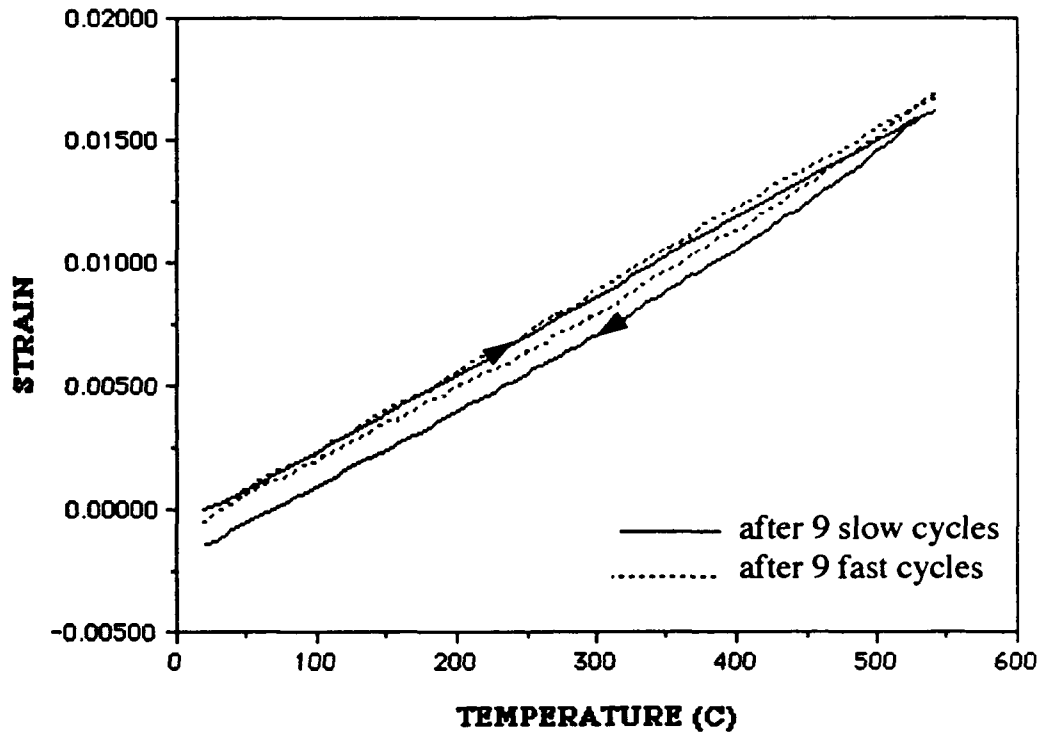
Figure 4.11 : Thermal strain response during the tenth cycle of the unidirectionally reinforced MMC with transversely oriented fibers following nine slow cycles (0.89°C/min, heating; 0.25°C/min, cooling) and nine fast cycles(17.33°C/min, heating and cooling).

1. LTTL MMC Cycled to 540°C

The middle layers of the LTTL sample have transversely oriented fibers. The unidirectionally reinforced MMC with the fibers oriented transversely showed a response similar to a monolithic aluminum sample, while the longitudinal orientation resulted in dramatic departures of the thermal strain from that of the

31

monolith. From this it is inferred that the strain response of the crossplied MMCs will be dominated by the longitudinal layers, especially since the stiffness of the longitudinal layers is much greater. The response of the LTTL in thermal cycling is similar to the unidirectionally reinforced longitudinal MMC, in its general characteristics, but with a somewhat larger CTE (Table 1) due to a smaller volume fraction of longitudinally oriented fibers. The response for the first and second thermal cycle to 540°C is shown in Figure 4.12.
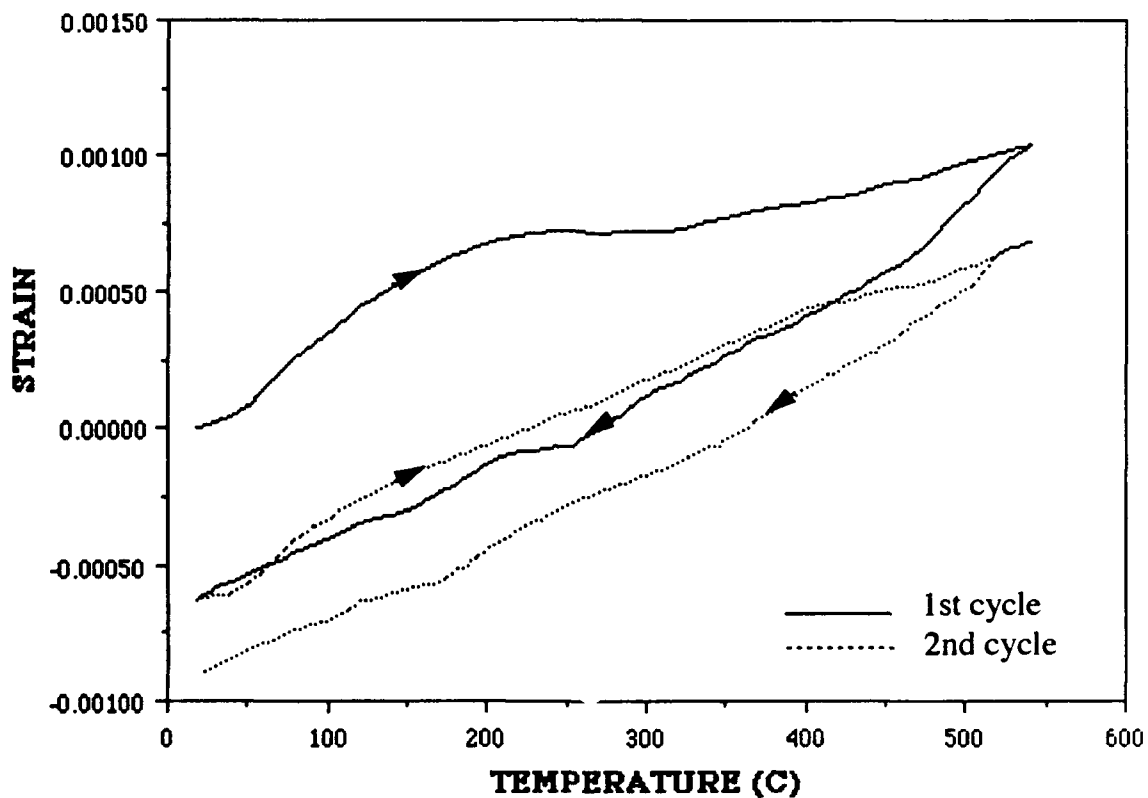
Figure 4.12 : Thermal strain response of the LTTL MMC during the first and second thermal cycles to 540°C.

TABLE 1. MEASURED CTE VALUES OVER THREE TEMPERATURE RANGES

SAMPLE	FIBER ORIENTATION	CYCLE #	CTE x 10^{-6}/°C		
			50-100°C	150-200°C	400-500°C
UNIDIRECTIONALLY REINFORCED	LONGITUDINAL FIBER REINFORCEMENT	1	3.52	1.57	0.50
		2	3.54	0.79	1.21
		10	6.83	4.09	-1.30
		10*	7.10	4.05	-0.83
	TRANSVERSE FIBER REINFORCEMENT	1	28.16	26.76	28.84
		2	27.92	28.07	30.29
		10	31.60	29.33	31.05
		10*	33.13	30.53	31.08
4-PLY CROSSPLIED	LTTL STACKING SEQUENCE	1	5.76	2.38	1.43
		2	5.17	2.05	1.88
		10	12.33	13.4	8.57
		10*	5.53	2.57	1.31
	TLLT STACKING SEQUENCE	1	4.79	1.98	0.51
		2	3.87	1.16	1.29
		10	4.71	1.38	4.32
		10*	4.95	2.33	0.51

All CTE values were calculated during thermal cycles with a heating rate of 0.89°C/min.

* indicates nine cycles at a heating rate of 17.33°C/min prior to the cycle in which the CTE value was calculated.

Several familiar features are exhibited such as the hysteresis between heating and cooling segments of each cycle and the residual compressive strain present at the end of each cycle. Again the residual compressive strain experienced after the second cycle is less than that of the first. The explanation for the thermal strain response is as follows. Upon initial heating the tensile residual stress present in the matrix aids in expansion. The CTE measured in the 50-100°C range is about 5.8×10^{-6}/°C, which is larger than the initial CTE in the unidirectional longitudinal sample. The residual stress state in this four-ply composite is tensile in both the longitudinal and transverse layers as shown earlier by Tsai [Ref. 5]. The initial increase in the CTE can be rationalized as being due to a smaller effective constraint that longitudinally oriented fibers apply. The transverse layers tend to expand more, giving an overall increase in the CTE. As the temperature rises, compressive stress that is built up in the longitudinal layers is also induced in the transverse layers, and the initial relatively unconstrained expansion of the transverse layers is now limited. Near 200°C the curve flattens temporarily indicating that the compressive stresses in the MMC have built to a magnitude large enough to limit expansion. However, the curve then exhibits a positive slope at higher temperatures. As the temperature continues to rise, the compressive stress that develops in the longitudinal plies is overcome by the tendency to expand that the central transverse layers exhibit. These two competing mechanisms (i.e. compressive stress in the longitudinal layers limiting expansion, and thermal expansion in the transverse layer) determine the behavior at higher temperatures. The effectiveness of the longitudinal layers in controlling the high temperature behavior is expected to be larger, for the same fiber volume fraction, when the longitudinal layers are in the center.

Upon cooling the compressive stress present is quickly relieved and tensile stress again builds in the composite. At the end of the cycle a compressive residual

strain is noted and is attributed to compressive creep and yielding which occurs in the heating segment at the higher temperatures. The second cycle shows features similar to the unidirectionally reinforced longitudinal MMC in that the flattening of the curve at higher temperatures does not occur. This is also attributed to a larger tensile stress present at the start of the second cycle than was present at the start of the first. The smaller compressive residual strain shown at the end of the second cycle further supports the presence of a larger tensile stress at the start of the second cycle.

The tenth cycles of two LTTL MMCs, slowly cycled and rapidly cycled for nine cycles, are shown in Figure 4.13. Both curves are nearly linear over the entire cycle, however the slowly cycled sample shows a much greater CTE.

The larger CTE displayed during the tenth slow cycle as compared with that during the first cycle (Figure 4.12) is directly attributable to interfacial debonding as observed in Figure 4.7. In the presence of substantial interfacial shear, the compressive creep at higher temperatures, and therefore the residual plastic strain is expected to be lower. However, we observed a larger residual plastic strain after the tenth cycle than after one cycle. This can be attributed to additional interfacial failure which occurs during the tenth cycle, resulting in matrix contraction (springback) to relieve stresses. During the tenth cycle following nine rapid cycles, the CTE and the residual plastic strain are much smaller than those of the tenth slow cycle, this supports the hypothesis that the larger CTE and residual plastic strain in the tenth slow cycle are results of interfacial failure.
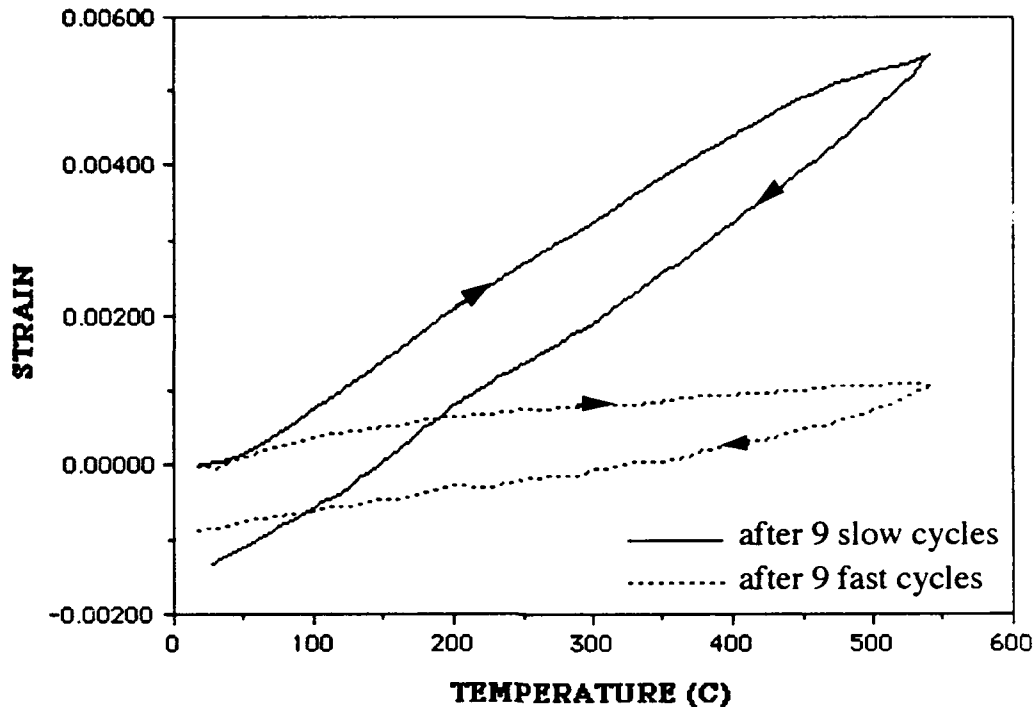
Figure 4.13 : Thermal strain response during the tenth cycle of the LTTL MMC following nine slow cycles (0.89°C/min, heating; 0.25°C/min, cooling) and nine fast cycles(17.33°C/min, heating and cooling).

2. TLLT MMC Cycled to 540°C

In this orientation the central longitudinal layers should dominate the strain response due to their greater stiffness than the outer transverse plies. The response of the first and second thermal cycles is shown in Figure 4.14.

Once again an initial CTE larger than that experienced in the unidirectional longitudinal was observed and can be attributed to the rapid expansion of the transverse layers. Once the compressive stress builds in the transverse layers from the effect of ply constraint of the longitudinal layers the initial expansion tapers off, and the CTE slope begins to flatten. At a temperature of 220°C the slope is

approximately zero and maintains this value through the end of the heating segment. This temperature is lower than the temperature at which the strain response of the unidirectionally reinforced MMC leveled off (~260°C), and can be attributed to the large compressive stresses induced into the transverse layers by the longitudinal layers. The corresponding tensile stress induced by the transverse layers on the longitudinal layers is very small because $E_{LONG} >> E_{TRANS}$. This is different from the LTTL response behavior which showed a small positive slope in the elevated temperature region of the first heating cycle.
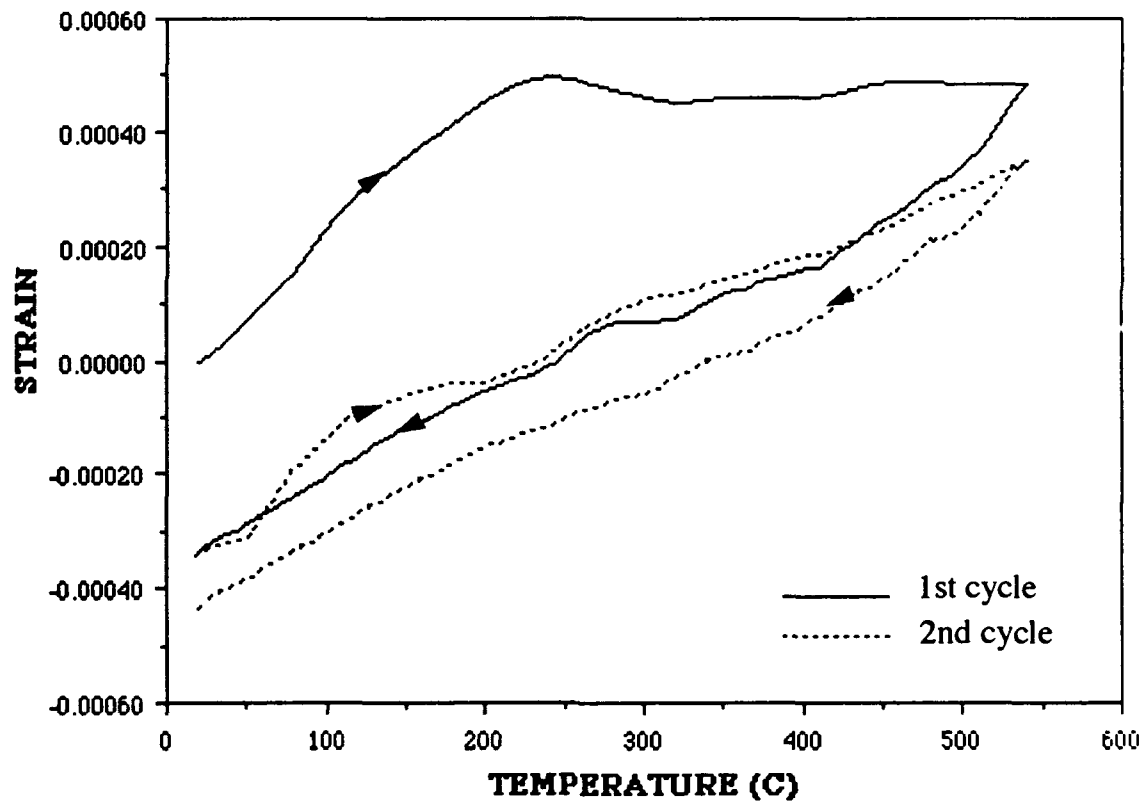

Figure 4.14 : Thermal strain response of the TLLT MMC during the first and second thermal cycles to 540 °C.

Upon cooling the compressive stress is quickly relieved and tensile stress builds throughout the remainder of the cooling cycle. A large residual compressive strain is again noted at the end of the first cycle which is attributed to the compressive yielding and compressive creep which occurs in the higher temperatures of the heating segment.

The second cycle shows no flattening of the curve which indicates a larger tensile stress present at the start of the cycle as previously explained. The smaller residual plastic strain evident at the end of the second cycle indicates less compressive yielding and compressive creep occurring throughout the second cycle.

Figure 4.15 compares the tenth slow cycle and the tenth fast cycle. Again there are some familiar features present in the curves, however there is also a substantial difference in the response of the slow and fast cycled samples. The slow cycled sample shows an initial expansion followed by a flattening of the curve indicating the compressive stress is large enough to limit expansion. As continued heating occurs the curve again returns to a large positive slope. In the fast cycled sample the slope is initially steeper but once the compressive stress builds and the curve flattens a constant slope is maintained throughout the remainder of the heating cycle. Upon cooling the same sequence of events is followed, that being the initial compressive stress aided contraction followed by the building of tensile stress through the remainder of the cooling cycles. At the end of the cycle a slightly larger compressive residual strain is observed in the slow cycled sample. The difference shown between the two curves again can be the effects of the damage occurring at the different thermal rates. These different damage mechanisms need further study.
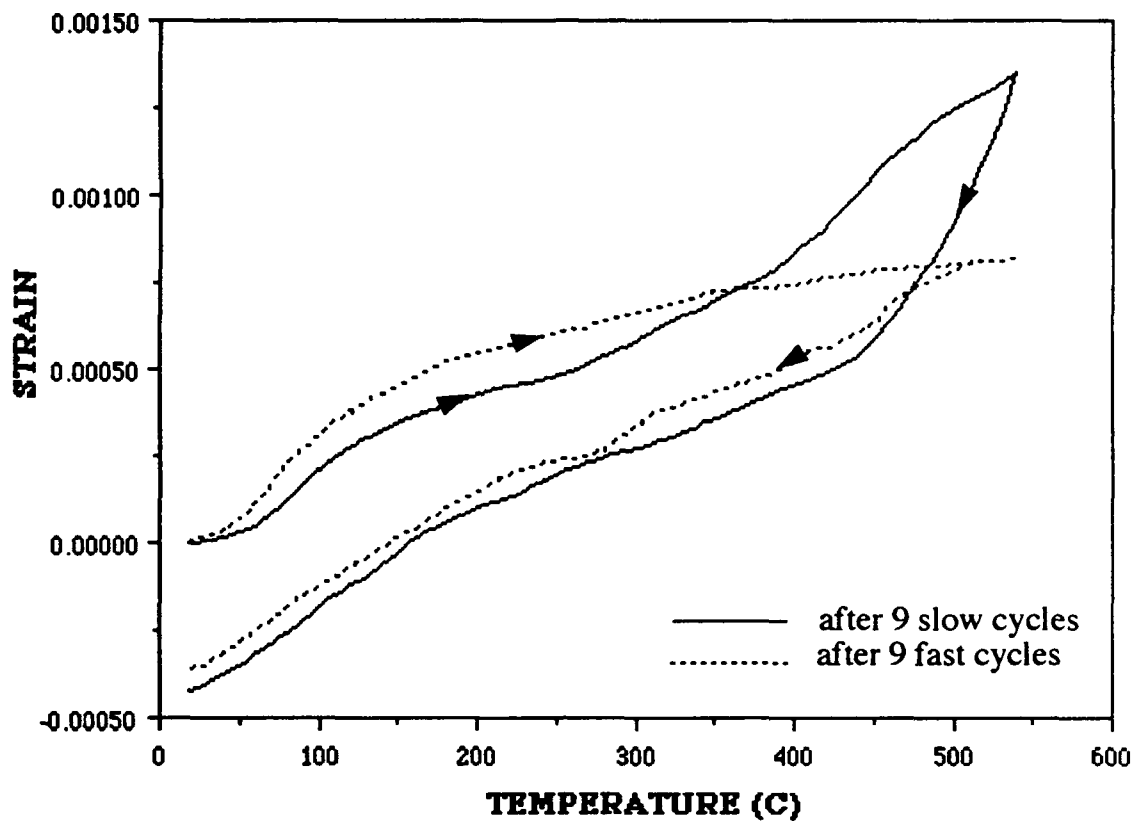
Figure 4.15 : Thermal strain response during the tenth cycle of the TLLT MMC following nine slow cycles (0.89°C/min, heating; 0.25°C/min, cooling) and nine fast cycles(17.33°C/min, heating and cooling).

C. THERMAL RATE DEPENDENCE OF THE STRAIN RESPONSE

It has been shown in the previous section that damage occurring over a period of ten cycles to 540°C can affect the strain response of the composite. However due to the number of cycles and the severity of the temperature range investigated it is difficult to ascertain from the previous experiments whether time dependent mechanisms were contributing to the strain response. To explore this possibility a unidirectionally reinforced longitudinal sample was heated at an effective rate of

0.15°C/min (as compared to 0.89°C/min, previously) to a maximum temperature of 100°C. By slowing down the heating rate, more time was allowed for stress relaxation to occur through time dependent mechanisms. The thermal strain response is shown in Figure 4.16.

The initial response is similar to the unidirectional longitudinal cycle to 540°C at 0.89°C/min shown in Figure 4.2. The important difference to note between the two curves is that some flattening of the strain response occurs at a much lower temperature (~ 80°C, vice ~260°C at 0.89°C/min) in Figure 4.16 due to the much slower heating rate. This indicates that the tensile residual stress present has been relieved and that compressive stress has already started to build. This is further substantiated by the small net compressive residual strain shown at the end of the first cycle.

The behavior during the second cycle is different from any previously noted, in that although the strain hysteresis is still present, the residual plastic strain at the end of the cycle has disappeared or is too small to be measured by the equipment being used. This can primarily be attributed to the absence of plastic yielding during the second cycle due to a larger residual tensile stress state before the start of the second cycle. The steeper slope during the second heating segment (compared with he first heating segment) further supports this. Although no residual plastic strain is present after the second cycle due to an absence of plastic strain, a hysteresis still exists between the heating and cooling segments of this cycle. This can be attributed directly to the tensile residual stress present in the matrix, which is enhanced due to matrix hardening.
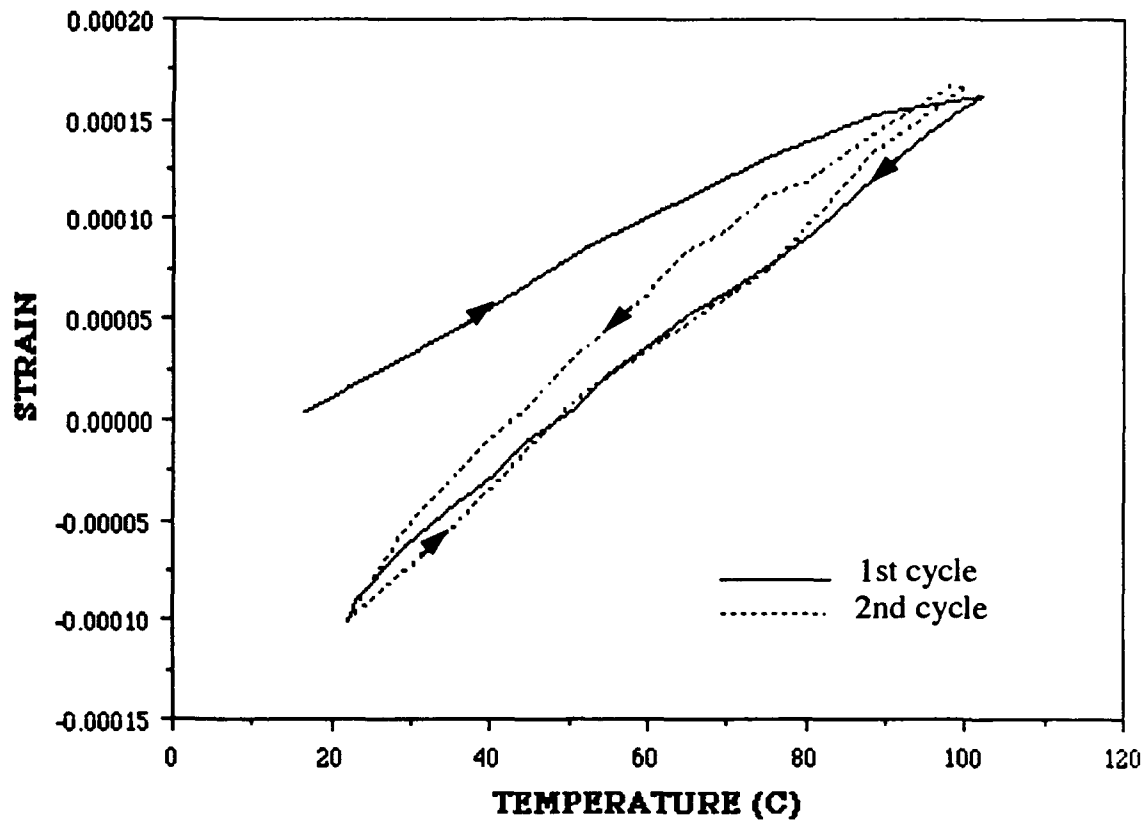
Figure 4.16 : Unidirectionally reinforced longitudinal MMC cycled at a rate of 0.15°C/min.

To further investigate the time dependent nature of the thermal strain response, the behavior of the unidirectionally reinforced longitudinal composite was investigated at several isothermal temperatures after various heating rates were used to reach the isothermal temperature. By varying the heating rate, the time dependent stress relaxation mechanisms can either be allowed to occur (slow heating rate) or be severely curtailed (rapid heating). If there is enough residual stress present in the composite once the isothermal holding temperature is reached, then it is possible to measure the strain behavior as a function of time at that temperature. The strain vs. time plots resemble creep behavior under a decreasing residual stress state with no

external stress applied to the composite. The results of this experiment are shown in Figure 4.17.
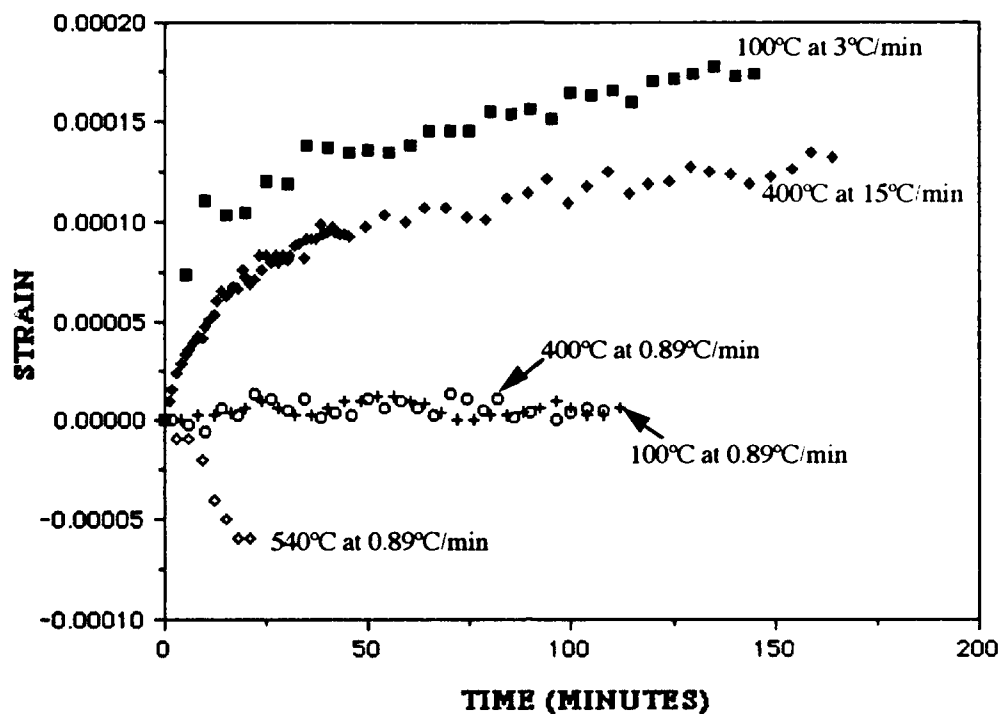
Figure 4.17 Isothermal strain response of unidirectionally reinforced longitudinal composites at various heating rates and isothermal holding temperatures.

It is evident from Figure 4.17 that upon slow heating (0.89°C/min) no strain is observed under isothermal conditions at 100°C and 400°C. Based upon Figure 4.2, we would expect some tensile stress to be present at 100°C and therefore some tensile creep, while some compressive stress should be present at 400°C resulting in some compressive creep. However, during slow heating, stress relief mechanisms occur continuously, resulting in very small stresses at the isothermal hold temperatures and consequently no measurable creep. When the heating rate is increased to 3°C/min, an isothermal hold at 100°C show significant tensile creep, as

expected. Although compressive creep is expected at 400°C, the faster heating rate (15°C/min) results in slower relief of the initial tensile residual stress, thereby leaving some tensile residual stress at 400°C. This residual stress results in the tensile creep seen in Figure 4.17. At an isothermal hold temperature of 540°C, however, with the slow heating rate (0.89°C/min) compressive creep is observed. This signifies that the compressive residual stresses that are generated at higher temperatures are so large that they are not completely relieved at the heating rate of 0.89°C/min. Thus the creep strain obtained under isothermal conditions in Al/Gr composites reflect the residual stress state in the matrix at the temperature of interest, prior to the isothermal hold. Therefore, an appropriate constitutive model can potentially be utilized to determine the stress state at any temperature from the total creep strain at that temperature. Future work will concentrate on the development of this model.

V. CONCLUSIONS

The thermal strain response of two 6061 aluminum-P100 graphite fiber reinforced composites (unidirectional and 0/90/90/0 lay ups) was studied, under thermal cycling conditions, up to 540°C. The strain response along the longitudinal direction (parallel to the fibers) showed strain hysteresis (which is attributed to residual stress in the matrix) and residual plastic strain after cycling (which is attributed to matrix plastic yielding and creep deformation). Both hysteresis and the residual strain diminished with further cycling. This is believed to be the result of plastic deformation and work hardening in the matrix which changes its residual stress state. On subsequent cycling damage accumulation in the form of fiber/matrix interface shear, fiber cracking, and matrix cracking, serves to alter the strain response. Thermal cycling of transversely oriented, unidirectionally reinforced composites showed very limited amounts of hysteresis and residual strain, but appeared similar to the behavior of monolithic aluminum over the entire range of temperatures. Hysteresis and residual plastic strain have been attributed to the small tensile residual stress that exists in the transverse direction (i.e. perpendicular to the fiber) in these composites.

The effect of ply constraints was studied in cross-plied composites with lay ups of LTTL (0/90/90/0) and TLLT (90/0/0/90), and 40 percent fiber volume. The overall behavior is similar to that of the longitudinal unidirectionally reinforced composite, although significant differences between the strain responses of the two lay ups were noticed. This is due to the different ply constraints present in the two lay ups. The LTTL lay up generally showed larger deformations while the TLLT lay up more closely resembled the unidirectionally reinforced composite, in the longitudinal orientation.

The thermal strain response of these composites was also found to have significant dependence on the heating rate. This is because the heating rate strongly affects the matrix residual stress state at any given temperature. The dependence of thermal strain on heating rates was clearly shown by the isothermal holds at 100°C and 400°C after heating to both temperatures at two very different rates. With the slower heating rates, no variation of strain with time was seen at the isothermal hold, whereas, with the faster rates, a variation in strain with time was seen, resulting in curves similar to primary creep curves without the application of external stresses. Creep strain in these cases occurred solely due to the presence of residual stresses that were themselves continually diminishing. With further quantification of this method, the residual stress state of the composite, upon reaching the isothermal holding temperature, may be determined.

APPENDIX

The data acquisition program was originally written by Tom Kellogg and Robert Hansen in May of 1990. Several changes were made to the program during the current research to obtain the desired output, and to facilitate easier data storage and retrieval.

The Hewlett Packard data acquisition unit receives an input in the form of millivolts from an extensometer and from the platinum-platinum/10% rhodium thermocouple which is used to control the dilatometer furnace temperature. Since the thermocouple's response is non-linear over the temperature ranges investigated, a linearization routine is incorporated into the program. This routine provides temperature readings within one degree of the actual sample temperature.

Prior to starting the acquisition program, the dilatometer sample should be inserted into the sample holder and should be allowed to stabilize to the new environment for at least fifteen minutes. Once the program is started it prompts the user for information about the setting of the "T Range" and the "Expansion Multiplier" settings on the dilatometer. The "T Range" must be set to 1500°C and the "Expansion Multiplier must be on the 0.2 setting. The dilatometer can be run on any setting with minor modifications to the data acquisition program.

After the prompts are finished, the program runs through an averaging routine which measures the sample 11 times over an 11 second period, and uses the average of these readings for the reference point for subsequent extensions measured during thermal cycling. The final input necessary from the user is the frequency at which the measurements are recorded. Once this sample rate is input the data acquisition program will continue to run until the specified number of measurements is completed.

The program used is shown on the following three pages.

```
10!                    RE-STORE "DILAT1"
20!                       JUNE 1 ,1992
30!***********************************************************************
40! THIS PROGRAM DOES COLLECTS OUTPUT IN THE FORM OF MILLIVOLT READINGS FROM THE
     ORTON DILITOMETER.
50!***********************************************************************
60!    Written 05-09-90 by Kellogg/Hansen
70!    Modified 04-23-92 by Wiest
80!***********************************************************************
90!    T range switch on the dilatometer must be set for 1500 C.
100!   EXPANSION MULTIPLIER MUST BE SET FOR .2
110!***********************************************************************
120   DIM Temp(5001),Extens(5001),Ext(5001)
130   INPUT "1=NEW RUN    2=RECALL   3=QUIT",Pick
140   IF Pick=1 THEN GOTO 170
150   IF Pick=2 THEN GOTO 1210
160   IF Pick=3 THEN GOTO 1340
170   INPUT "IDENTIFY THE RUN NAME",F_name$
180   MASS STORAGE IS ":CS80,700"
190   CREATE BDAT F_name$,4271,20
200   ASSIGN @Path1 TO F_name$
210   INPUT "1=1 RUN 100C   2=2 RUNS 100C   3=1 RUN 540C    4=TEST",Cycl
220   IF Cycl=1 THEN N=800
230   IF Cycl=2 THEN N=1300
240   IF Cycl=3 THEN N=1000
250   IF Cycl=4 THEN N=11
260   T_start=0
270   INPUT "Is the T range switch set for 1500 C (1=yes)?",X
280   INPUT "Is the expansion multiplier set for 0.2 (1=yes)?",Xx
290   T_start=0
300   T_end=10
310   T_total=T_end-T_start
320   T_0=TIMEDATE
330   OUTPUT 709;"CLR"
340   OUTPUT 709;"USE 000"
350   OFF KEY
360   Sum=0
370   FOR I=0 TO 10
380     REPEAT
390       T_1=(TIMEDATE-T_0)
400     UNTIL T_1>=(T_total/11)*I
410     OUTPUT 709;"CONFMEAS DCV, 201"
420     ENTER 709;Extens(I)
430     Sum=Sum+Extens(I)
440     OUTPUT 709;"CONFMEAS DCV, 200"
450     ENTER 709;Tmv
460     PRINT Sum,Tmv
470   NEXT I
```

```
480     Avg=Sum/I
490     PRINT Avg
500     INPUT "Specify interval between readings, sec",W
510     Y=Avg
520     T_start=0
530     T_end=W*N
540     T_total=T_end-T_start
550     T_0=TIMEDATE
560     OUTPUT 709;"CLR"
570     OUTPUT 709;"USE 000"
580     OFF KEY
590     FOR I=0 TO N
600       REPEAT
610         T_1=(TIMEDATE-T_0)
620       UNTIL T_1>=(T_total/N)*(I)
630       OUTPUT 709;"CONFMEAS DCV, 201"
640       ENTER 709;Extens(I)
650       OUTPUT 709;"CONFMEAS DCV, 200"
660       ENTER 709;Tmv
670       IF Tmv<=.00032 THEN
680         Tem=Tmv*1000*1.35
690       END IF
700       IF Tmv>.00032 THEN
710         Tem=Tmv*1000*1.425
720       END IF
730       IF Tmv>.000377 THEN
740         Tem=Tmv*1000*1.44
750       END IF
760       IF Tmv>.00045 THEN
770         Tem=Tmv*1000*1.46
780       END IF
790       IF Tmv>.000536 THEN
800         Tem=Tmv*1000*1.485
810       END IF
820       IF Tmv>.0007 THEN
830         Tem=Tmv*1000*1.55
840       END IF
850       IF Tmv>.0010306 THEN
860         Tem=Tmv*1000*1.6
870       END IF
880       IF Tmv>.001349 THEN
890         Tem=Tmv*1000*1.623
900       END IF
910       IF Tmv>.00199999 THEN
920         Tem=Tmv*1000*1.634
930       END IF
940       IF Tem<=-.807449459 THEN
950         GOTO 1170
```

```
960      END IF
970      IF Tem<=.645 THEN
980        Temp(I)=-293.0851+SQRT(343595.5186+425531.92*Tem)/2
990      END IF
1000     IF Tem>.645 THEN
1010       Temp(I)=-569.4974+SQRT(1138.9948*1138.9948+4*(6953.1129+181143.012*Tem
))/2
1020     END IF
1030     IF Tem>1.42 THEN
1040       Temp(I)=-1089.3397+SQRT(2178.67993*2178.67993+4*(39301.554+303186.5*Te
m))/2
1050     END IF
1060     IF Tem>2.323 THEN
1070       Temp(I)=-1810.7164+SQRT(3621.43284*3621.43284+4*(105298.52+461041.96*T
em))/2
1080     END IF
1090     IF Tem>3.26 THEN
1100       Temp(I)=-2842.327+SQRT(5684.654*5684.654+4*(231740.473+675675.676*Tem)
)/2
1110     END IF
1120     IF Tem>4.234 THEN
1130       Temp(I)=-3577.845+SQRT(7155.68997*7155.68997+4*(346742.98+822386.42*Te
m))/2
1140     END IF
1150     Ext(I)=2*(Extens(I)-Y)
1160     OUTPUT @Path1;Temp(I),Ext(I)
1170     PRINT USING "4D,2X,4A,2X,DD.4D,X,2A,2X,2A,X,4D.DD,2X,3A,X,DD.7D,X,A,2X,2
D.7D,X,2A";I,"TEMP";Tem;"mV","C=";Temp(I),"EX=";Extens(I),"V",Ext(I);"in"
1180  NEXT I
1190  ASSIGN @Path1 TO *
1200  GOTO 130
1210  INPUT "WHICH FILE SHOULD BE RETRIEVED?",F_name$
1220  MASS STORAGE IS ":CS80,700"
1230  INPUT "HOW MANY DATA POINTS SHOULD BE RETRIEVED?",N
1240  ASSIGN @Path TO F_name$
1250  FOR I=1 TO N
1260    ENTER @Path;Temp(I),Ext(I)
1270  NEXT I
1280  ASSIGN @Path TO *
1290  FOR I=1 TO N
1300    PRINT Temp(I),Ext(I)
1310  NEXT I
1320  PRINTER IS 1
1330  GOTO 130
1340  END
```

LIST OF REFERENCES

1. Chawla, K. K., Composite Materials Science and Engineering, pp. 1-5, Springer-Verlag New York Inc., 1987.

2. Rossi, R. C., Pepper, R. T., Upp., J. W. and Riley, W. C., Development of Aluminum-Graphite Composites, "*American Ceramic Society Bulletin*, v.50, no. 5, pp. 484-487, May 1971.

3. National Aeronautics and Space Administration Technical Paper - 2612, *Effects of Thermal Cycling on Graphite-Fiber-Reinforced 6061 Aluminum*, by G. A. Dries and S. S. Tompkins, p. 3, October 1986.

4. Dutta, I., "Thermal Fatigue of P100 Gr - 6061 Al Composite," Progress Report #2 to NWSC Crane, Indiana, April 30, 1990.

5. Tsai, S., Mahulikar, D., Marcus, H.L., "Residual Stress Measurements on Al-Graphite Composites Using X-ray Diffraction," *Materials Science and Engineering*, v. 47, no. 2, pp. 145-149, February 1981.

6. Mitra, S., Dutta, I., Hansen, R. C., "Thermal Cycling Studies of a Cross-plied Graphite Fibre-reinforced 6061 Aluminum Composite Laminate," *Journal of Material Science*, v. 26, pp. 6223-6230, 1991.

7. Park, H. S., *Residual Stress Measurement and Microstructural Characterization of Graphite Aluminum Metal Matrix Composites*, PhD Dissertation, University of Texas at Austin, August 1989.

8. Dries, G. A., and Tompkins S. S., Development of Stable Composites of Graphite-Reinforced Aluminum and Magnesium, 12th Conference on Composite Materials and Structures, DOD/NASA Cocoa Beach, Fl., January 20-21, 1988.

9. Wolff, E. G., Min, B. K., Kural, M. H., "Thermal Cycling of a Unidirectional Graphite-Magnesium Composite," *Journal of Material Science*, v. 20, pp. 1145, 1984.

10. Tompkins, S. S., Dries, G. A., "Thermal Expansion Measurements of Metal Matrix Composites," *Testing Technology of Metal Matrix Composites, ASTM STP 964*, pp. 248-258, P. R. DiGiovanni and N. R. Adsit, Eds., American Society for Testing and Materials, Philadelphia, 1988.

11. Kural, M. H. and Min, B. K., "The Effects of Matrix Plasticity on the Thermal Deformation of Continuous Fiber Graphite/Metal Composites, "*Journal of Composite Materials*, v. 18, pp. 519-533, November 1984.

12. Koss, D. A., and Copley, S. M., "Thermally Induced residual Stresses in Eutectic Composites," *Metallurgical Transactions*, v. 2, pp. 1559, March 1971.

13. Garmong, G., "Elastic-Plastic Analysis of Deformation Induced by Thermal Induced by Thermal Stress in Eutectic Composites: I. Theory," *Metallurgical Transactions*, v. 5, pp. 2183-2190, October 1974.

14. Khan, I. H., "The Effect of Thermal Exposure on the Properties of Aluminum-Graphite Composites," *Metallurgical Transactions A*, v. 7A, pp. 1281-1289, September 1976.

15. Zong, G. S., Rabenberg, L., Marcus, H. L., "In Situ SEM Thermal Fatigue of Al/Graphite Metal Matrix Composites," Fundamental Relationships Between Microstructure and Mechanical Properties of Metal Matrix Composites, Conference Proceedings, The Minerals, Metals And Materials Society, pp. 289-299, 1990.

INITIAL DISTRIBUTION LIST

1. Defense Technical Information Center   2
   Cameron Station
   Alexandria, Virginia   22304-6145

2. Library, Code 52   2
   Naval Postgraduate School
   Monterey, California   93943-5002

3. Department Chairman, Code ME/KK   2
   Department of Mechanical Engineering
   Naval Postgraduate School
   Monterey, California   93943-5002

4. Professor I. Dutta, Code ME/DU   1
   Department of Mechanical Engineering
   Naval Postgraduate School
   Monterey, California   93943-5002

5. Professor S. Mitra, Code ME/MT   1
   Department of Mechanical Engineering
   Naval Postgraduate School
   Monterey, California   93943-5002

6. Naval Engineering Curricular Office, Code 34   2
   Naval Postgraduate School
   Monterey, California   93943-5002

7. Kevin G. Beasley   1
   Naval Weapons Support Center
   Electronic Development Department
   Crane, Indiana   47522

8. Robert E. Morgan   1
   NAWC Aircraft Division Indianapolis
   6000 E. 21st Street
   Indianapolis, Indiana   46219-2189

9. Anthony D. Wiest   1
   11961 Holly View Drive
   Woodbridge, Virginia   22192

10. Program manager, NA&ME   1
    Commandant (G-MTH-2)
    U. S. Coast Guard
    2100 2nd St. SW
    Washington, DC   20593

11. Coast Guard Law Library   1
    U. S. Coast Guard
    2100 2nd St. SW
    Washington, DC   20593